

Open Research Online

The Open University's repository of research publications and other research outputs

Morphological evidence for geologically young thaw of ice on Mars: a review of recent studies using high-resolution imaging data

Journal Item

How to cite:

Balme, Matthew; Gallagher, C. J. and Hauber, E. (2013). Morphological evidence for geologically young thaw of ice on Mars: a review of recent studies using high-resolution imaging data. *Progress in Physical Geography*, 37(3) pp. 289–324.

For guidance on citations see [FAQs](#).

© 2013 The Authors

Version: Accepted Manuscript

Link(s) to article on publisher's website:

<http://dx.doi.org/doi:10.1177/0309133313477123>

<http://ppg.sagepub.com/content/37/3/289.full.pdf+html>

Copyright and Moral Rights for the articles on this site are retained by the individual authors and/or other copyright owners. For more information on Open Research Online's data [policy](#) on reuse of materials please consult the policies page.

oro.open.ac.uk

Morphological evidence for geologically young thaw of ice on Mars: a review of recent studies using high resolution imaging data

Journal:	<i>Progress in Physical Geography</i>
Manuscript ID:	PPG-11-080.R2
Manuscript Type:	Main Article
Keywords:	Mars, Thaw, Periglacial, Geomorphology, Permafrost
Abstract:	<p>Liquid water is generally only meta-stable on Mars today; it quickly freezes, evaporates or boils in the cold, dry, thin atmosphere (surface pressure is about 200 times lower than on Earth). Nevertheless, there is morphological evidence that surface water was extensive in more ancient times, including the Noachian Epoch (~ 4.1 Ga to ~ 3.7 Ga bp), when large lakes existed and river-like channel networks were incised, and early in the Hesperian Epoch (~ 3.7 Ga to ~ 2.9 Ga bp), when megafloods carved enormous channels and smaller fluvial networks developed in association with crater-lakes. However, by the Amazonian Epoch (~ 3.0 Ga to present), most surface morphogenesis associated with liquid water had ceased, with long periods of water sequestration as ice in the near-surface and polar regions. However, inferences from observations using imaging data with sub-meter pixel sizes indicate that periglacial landscapes, involving morphogenesis associated with ground-ice and/or surface-ice thaw and liquid flows, has been active within the last few million years. In this paper, three such landform assemblages are described: a high latitude assemblage comprising features interpreted to be sorted clastic stripes, circles and polygons, non-sorted polygonally patterned ground, fluvial gullies, and solifluction lobes; a mid-latitude assemblage comprising gullies, patterned ground, debris-covered glaciers and hill-slope stripes; and an equatorial assemblage of linked basins, patterned ground, possible pingos, and channel-and-scarp features interpreted to be retrogressive thaw-slumps. Hypotheses to explain these observations are explored, including recent climate change, and hydrated minerals in the regolith 'thawing' to form liquid brines at very low temperatures. The use of terrestrial analog field sites is also discussed.</p>

1
2
3
4
5
6
7
8
9
10
11
12
13
14
15
16
17
18
19
20
21
22
23
24
25
26
27
28
29
30
31
32
33
34
35
36
37
38
39
40
41
42
43
44
45
46
47
48
49
50
51
52
53
54
55
56
57
58
59
60

1 Liquid water is generally only meta-stable on Mars today; it quickly freezes, evaporates or
2 boils in the cold, dry, thin atmosphere (surface pressure is about 200 times lower than on
3 Earth). Nevertheless, there is morphological evidence that surface water was extensive in
4 more ancient times, including the Noachian Epoch (~ 4.1 Ga to ~ 3.7 Ga bp), when large
5 lakes existed and river-like channel networks were incised, and early in the Hesperian Epoch
6 (~ 3.7 Ga to ~ 2.9 Ga bp), when megafloods carved enormous channels and smaller fluvial
7 networks developed in association with crater-lakes. However, by the Amazonian Epoch (~
8 3.0 Ga to present), most surface morphogenesis associated with liquid water had ceased, with
9 long periods of water sequestration as ice in the near-surface and polar regions. However,
10 inferences from observations using imaging data with sub-meter pixel sizes indicate that
11 periglacial landscapes, involving morphogenesis associated with ground-ice and/or surface-
12 ice thaw and liquid flows, has been active within the last few million years. In this paper,
13 three such landform assemblages are described: a high latitude assemblage comprising
14 features interpreted to be sorted clastic stripes, circles and polygons, non-sorted polygonally
15 patterned ground, fluvial gullies, and solifluction lobes; a mid-latitude assemblage comprising
16 gullies, patterned ground, debris-covered glaciers and hill-slope stripes; and an equatorial
17 assemblage of linked basins, patterned ground, possible pingos, and channel-and-scarp
18 features interpreted to be retrogressive thaw-slumps. Hypotheses to explain these observations
19 are explored, including recent climate change, and hydrated minerals in the regolith ‘thawing’
20 to form liquid brines at very low temperatures. The use of terrestrial analog field sites is also
21 discussed.
22

Morphological evidence for geologically young thaw of ice on Mars: a review of recent studies using high resolution imaging data

1. Introduction

Data from the most recent Mars missions, such as NASA's *Mars Global Surveyor* (MGS; 1997-2006; Albee et al., 2001) and *Mars Reconnaissance Orbiter* (MRO; 2006 and ongoing; Zurek and Smrekar, 2007) and ESA's *Mars Express* (MEx; 2004 and ongoing; Chicarro et al., 2004), have revealed new evidence for recent geological activity on Mars (e.g., Malin et al., 2006; Marquez et al., 2004; McEwen et al., 2011). In particular, these missions have provided new insights to the geomorphic activity of water and ice on Mars. For example, one of the most significant results from the MGS mission was the observation of kilometre-scale gullies (Malin and Edgett, 2000) that were interpreted to have been created by flows of liquid water. Importantly, these gullies formed only in the last few million years (Reiss et al., 2004), rather than in Mars' more distant past (for a brief summary of Mars' geological timescale, evolution and ongoing research, see Bargery et al., 2011) when large scale hydrogeological activity was more common (Baker, 2001; Carr, 1987). This conclusion is important, for the geologically recent presence of liquid water at the surface both provides important information about the recent climate, and improves the chances that Mars could have supported life in refugia at or near the surface (e.g., Jakosky, 2007) in recent times.

21

22 The gullies, identified in MGS Mars Orbiter Camera (MOC) Narrow Angle images

23 with a spatial resolution of about 2 m per pixel, are generally interpreted as having

24 formed due to thaw of ice or snow (e.g., Balme et al., 2006; Costard et al., 2002;

25 Dickson and Head, 2009; Levy et al., 2009b). Since the end of the MGS mission in

26 2006, additional morphological indicators of thaw in Mars' recent past have been

27 identified in newer, even higher resolution imaging data. Much of these new data come

28 from the NASA High Resolution Imaging Science Experiment (HiRISE) instrument,

29 aboard the MRO spacecraft, with a spatial resolution of ~ 30 cm per pixel. These data

30 allow surface features to be identified that were either unseen or ambiguous in the MGS

31 images and such observations highlight the rapid pace at which martian geomorphology

32 is advancing.

33

34 In this paper, case studies from the literature (either drawn from a single work or as a

35 synthesis of several studies) are presented that utilize these new data, each study

36 documenting an assemblage of landforms interpreted to have formed by thaw of snow

37 and/or ground ice on Mars in the past few million years. The aim of this work is not to

38 review exhaustively the ice related landforms on Mars, but instead to demonstrate the

39 recent progress made (largely due to HiRISE data) in demonstrating that thaw has

40 played a role in shaping the martian surface in the last few million years. In particular,

recent work has suggested that ground-ice thaw might have shaped the surface, in addition to the melt of surface ice or snow proposed to play a major role in shaping or creating gullies (e.g., Levy et al., 2009b). The paper includes first a brief summary of relevant aspects of the martian climate, and a short description of the most common landforms thought to be indicative of near-surface ice (with or without thaw) on Mars. Three landforms assemblages, described in the recent literature as being indicative of thaw, are reviewed. The paper concludes by considering whether thaw on Mars is indicative of recent climate-warming events, or if other explanations, including the local depression of freezing points by the inclusion of salts in regolith materials and fluids, are more likely.

2. Water and the martian climate

Mars' current climate is cold and dry (e.g., Read and Lewis, 2004): the atmosphere is 95% CO₂ (Owen et al., 1977) and the mean annual surface temperature is ~ 210 K, although surface temperatures can range between 140 to 300 K (Kieffer et al., 1977). Atmospheric pressure is below 10 hPa (Hess et al., 1977), with column abundances of water less than 100 precipitable microns, even above the north polar ice cap in summer (Jakosky and Farmer, 1982). Mars' axial obliquity (currently ~26°; Laskar et al., 2004) means that high latitude winter temperatures are so low that CO₂ condenses from the

61 atmosphere to form a seasonal dry-ice cap that persists well into spring. Thus water on
62 Mars is today stable on multiyear timescales only in the solid state (liquid water can
63 persist briefly on Mars, even today, as discussed by Hecht, 2002) and even then only in
64 the coolest regions, such as steep, pole facing slopes at latitudes higher than about 25°
65 or in almost all terrains at latitudes higher than about 60° (Aharonson and Schorghofer,
66 2007; Schorghofer and Aharonson, 2005).

67
68 There is, however, strong morphological evidence that surface water was more
69 extensive in Mars' ancient Noachian (~ 4.1 Ga to ~ 3.7 Ga bp) and Hesperian (~ 3.7 Ga
70 to ~ 2.9 Ga bp) epochs than today, including valley networks, outflow channels and
71 palaeolakes (e.g., Ansan and Mangold, 2006; Baker, 2001; Carr, 1987; Irwin et al.,
72 2005; Mangold et al., 2004). Such observations have been interpreted as evidence for an
73 early warmer, wetter martian climate, in which liquid water was more stable (e.g.,
74 Craddock and Howard, 2002) although these interpretations are still widely debated and
75 it is not known whether Mars was actually 'warm and wet' or instead was 'cold and
76 wet' (e.g., Fairen, 2010; Fastook et al., 2012). Since the onset of the Amazonian Epoch
77 (~ 3.0 Ga to present), Mars' has been colder and dryer, and most of Mars' water is
78 thought to have been locked away as ice in the regolith, forming an extensive
79 cryosphere buried beneath dryer material (Carr, 2000) or exposed at the poles, although
80 large-scale volcanic, tectonic and fluvial events could have caused significant climate

excursions in the past by releasing large amounts of volatiles into the atmosphere (e.g., Baker et al., 1991).

Although the Amazonian is probably the driest and coldest of Martian epochs, there have been climate changes within the epoch relevant to the behaviour of water and ice. This is because unlike the Earth, Mars has no large moon to stabilise its rotation, so the martian axial obliquity has varied $\sim 15^\circ$ and 35° in cycles lasting $\sim 120,000$ years (see Figure 2, after Laskar et al., 2004). Furthermore, modelling has shown that Mars' mean obliquity changed from about 35° to about 25° about five million years ago (Laskar et al., 2004), perhaps defining a recent period in which insolation patterns have been atypical and which might have associated geomorphological consequences (e.g., Head et al., 2008), or even defining martian 'ice-ages' (Head et al., 2003). Hence we define "recent" in this paper as meaning the last ~ 20 ma, the period over which Mars' obliquity and eccentricity can be precisely modelled (Laskar et al., 2004), and during which there were both many obliquity cycles, and the systematic change in the mean obliquity about 5 ma ago.

Can the formation of different types of landforms and landscapes be associated with such recent changes in past climate? When trying to answer this question, it must be noted that the main way to determine *when* martian surfaces were formed is to examine

1
2
3
4
5
6
7
8
9 101 the size-frequency statistics of impact craters superposing them (e.g., Hartmann and
10 102 Neukum, 2001). Small and geologically recent features have few superposed impact
11
12 103 craters, and so are difficult to date in absolute terms (Hartmann, 2007). Major
13
14 104 uncertainties associated with craters smaller than 200 m are the effects of target
15
16 105 properties (e.g., Dundas et al., 2010a) and the possible contamination by secondary
17
18 106 craters (e.g., McEwen and Bierhaus, 2006). The accuracy of crater retention ages
19
20 107 obtained for small features might never be better than an order of magnitude (Hartmann,
21
22 108 2007), although this is good enough for many studies.
23
24
25
26 109
27
28 110 Furthermore, landforms on Mars need not have formed under the present day climate to
29
30 111 appear youthful but could be significantly older because, compared with the Earth, the
31
32 112 rate of erosion and burial is extremely low. Estimates of erosion rates on Mars show a
33
34 113 rapid decrease from 10^{-7} – 10^{-5} myr⁻¹ in Noachian terrains (characterized by rimless, flat-
35
36 114 floored craters and valley networks) to the exceedingly slow rates of 10^{-11} to 10^{-10} myr⁻¹
37
38 115 during the Hesperian and Amazonian periods (Golombek and Bridges, 2000). These
39
40 116 recent values are many orders of magnitude lower than terrestrial continental
41
42 117 denudation rates. Hence, martian surfaces that are millions of years old can appear
43
44 118 pristine. This is particularly important to consider when trying to link landforms and
45
46 119 landscape thought to have formed by thaw to the cyclic changes in Mars' orbital
47
48
49 120 parameters over the past few million years (Kreslavsky et al., 2008). Consequently it
50
51
52
53
54
55
56
57
58
59
60

1
2
3
4
5
6
7
8
9 121 might be difficult to differentiate from morphology alone between landforms decades or
10 122 centuries old, formed under present day conditions, and those created during different
11 123 obliquity and eccentricity (and perhaps climate) conditions, hundreds of thousands (or
12 124 even millions) of years ago.
13
14
15
16
17
18
19

126 3. Components of thaw-related martian landscapes

127 Much of the landscape of the northern plains of Mars, seen in Viking Orbiter images,
128 was ascribed to ‘periglacial’ modification based on their “grooved, mottled, knobby and
129 ridged morphologies” (Tanaka et al., 1992) and on the identification of apparent
130 thermokarst (e.g., Carr and Schaber, 1977; Costard and Kargel, 1995) and polygonally
131 patterned grounds in the highest resolution (up to 7.5m per pixel; Snyder and Moroz,
132 1992) Viking images (Lucchitta, 1981). It should be noted that the term ‘periglacial’ is
133 sometimes poorly defined in planetary science. We define ‘periglacial’ as *landforms or*
134 *landscapes shaped by transitory ice, generally inferring processes of freeze-thaw with a*
135 *seasonal or otherwise cyclical oscillation of water between a solid (frozen) and liquid*
136 *state*. The ages of ‘periglacial’ terrains seen in Viking images were poorly constrained
137 (Carr and Schaber, 1977; Lucchitta, 1981; Rossbacher and Judson, 1981) and the
138 evidence for thaw in the landscape was ambiguous. Newer studies using modern
139 datasets with higher spatial resolution (e.g. from HiRISE and MOC) have identified a
140 variety of possibly thaw-related landscapes, and it has been inferred that many are

141 geologically recent. The landforms that most often compose such landscapes, including
142 both periglacial landforms in the strict sense and other landforms related to ice and thaw
143 of ice that are found in association with them, are described below. Table 1 summarises
144 these components and Figure 3 shows examples of landforms in which liquid water
145 derived from thaw or snowmelt is thought to have played a formative role.

147 **3.1 Polygonally patterned ground**

149 Polygonised ground is widespread on Mars. While polygons might be the result of
150 desiccation (El Maarry et al., 2010) and other processes such as tectonic uplift, rock
151 jointing, or convection in a lava lake (for a comprehensive overview of proposed
152 mechanisms see the appendix and cited references in Levy et al., 2009a), many small-
153 scale polygons with diameters of meters to tens of meters are closely analogous to
154 terrestrial thermal contraction polygons based on several comparative criteria (Mellon,
155 1997). Furthermore, their distribution is strongly latitude-dependent (Levy et al., 2009a;
156 Mangold, 2005; Seibert and Kargel, 2001), implying a control by climatic or global
157 environmental factors. Levy et al. (2010) compared polygons on Mars with terrestrial
158 analogues in Arctic and Antarctic environments, examining polygon plan-form
159 morphology, microtopography, sediment sorting patterns, landform ages, and
160 relationships between polygons and other landforms (e.g., gullies, desert pavements,

1
2
3
4
5
6
7
8
9 161 boulder halos). They concluded that martian polygons are probably sand wedge or
10
11 162 sublimation polygons, rather than ice-wedge polygons. This conclusion is not
12
13 163 supportive of the concept of freeze/thaw cycles as factors in recent Martian
14
15 164 geomorphology. However, making a distinction between different types of thermal
16
17 165 contraction polygons on the basis of remote-sensing and in situ imagery and derived
18
19 166 topographic information alone is problematic on Earth, and more so on Mars (Ulrich et
20
21 167 al., 2011).
22
23

24 168

25 169 ***3.2 Sorted patterned ground (stripes, circles and lobate forms)***

26
27
28
29 170

30
31 171 Possible spatial sorting of regolith into fine and coarse particle size domains on martian
32
33 172 mid-latitude crater walls has been observed by Hauber et al. (2011a) and Mangold
34
35 173 (2005), where alternating stripes of bright and dark albedo surfaces are oriented down
36
37 174 slope. Stronger evidence for sorted landforms comes from observations where clasts can
38
39 175 be resolved: clastic stripes, circles and labyrinths at high latitude are described by
40
41 176 Gallagher et al. (2011) and Gallagher and Balme (2011). Sorted circles and polygons
42
43 177 have also been found at the margins of what appear to be fluvial flood-carved channels
44
45 178 near the equator (Balme et al., 2009). In addition to sorted stripes and circles, distinctive
46
47 179 clastic and non-clastic lobes have been found on the same impact crater walls
48
49 180 (Gallagher and Balme, 2011; Gallagher et al., 2011; Johnsson et al., 2011), as shown in
50
51
52
53
54
55
56
57
58
59
60

Figure 3. Together, these observations are consistent with an origin by a combination of cryoturbation, frost creep, solifluction, sorting and gravitational slumping.

Simple clastic patterns might occur without the presence of water, through gravitational slumping of clasts into thermal contraction cracks (e.g., Levy et al., 2009a; Mellon, 1997), and sorting driven by seasonal deposition of CO₂ frost ‘locking’ boulders in place while the ground contracts beneath has also been proposed (Orloff et al., 2012). However, such mechanisms arguably explain neither the full variety nor the spatial associations of sorted morphologies observed as comprehensively as does a genesis involving freeze-thaw processes.

3.3 Viscous flow features

Viscous flow features, widespread on Mars, are a family of landforms usually tens of kilometres in scale that were originally identified in Mariner and Viking images (e.g., Squyres, 1979) and include features descriptively termed lobate debris aprons, lineated valley fill, and concentric crater fill. Such features are not periglacial, but are instead probably glacial, so they are not in themselves indicators of thaw. Their distribution is confined to mid-latitudes (Milliken et al., 2003; Squyres and Carr, 1986) but relict forms (Hauber et al., 2008) and some crater-floor morphologies (Shean, 2010) indicate

201 a former extent towards latitudes lower than 30°. Their morphology was interpreted as
202 indicative of plastic deformation, and they were originally interpreted as rock glaciers
203 (Squyres, 1979). However, morphologic analysis (Hauber et al., 2008) and radar
204 measurements (Holt et al., 2008; Plaut et al., 2009) suggest that they consist of
205 relatively pure ice overlain by a protecting surface lag, hence debris-covered glacier is a
206 more appropriate term to describe them.

207

208 Higher resolution images show a preferential occurrence of smaller-scale (km) viscous
209 flow features (referred to as Glacier-like forms (GLFs) by Hubbard et al., 2011) on
210 pole-facing mid-latitude slopes of any type of relief (Milliken et al., 2003; Souness et
211 al., 2012). Their morphology, too, suggests plastic or superplastic deformation (Li et al.,
212 2005; Milliken et al., 2003), and so they also have been interpreted as debris-covered
213 glaciers (Head et al., 2010) or ‘dust glaciers’ (Hauber et al., 2011a). We use the term
214 debris-covered glaciers for these features, albeit following the rather generic definition
215 of rock glaciers as of Berthling (2011: , p. 105), who suggested that rock glaciers are
216 ‘the visible expression of cumulative deformation by long-term creep of ice/debris
217 mixtures under permafrost conditions’. In this context, ice could have been incorporated
218 in talus or dust from seasonal frost (Squyres, 1979) or by the direct incorporation of
219 ground ice (Lucchitta, 1984).

220

221 **3.4 *Small-scale Valleys***

222

223 While the ubiquitous creep of the ice-rich permafrost material on Mars does not require
224 liquid water to occur, some kilometre-scale fluvial valleys seem to be closely
225 associated with debris-covered glaciers (Dickson et al., 2009; Fassett et al., 2010;
226 Howard and Moore, 2011), being proglacial (a term usually formally applied to glacial
227 environments, but fitting the context of debris-covered glaciers as defined above),
228 situated down slope of the debris-covered glaciers, or supraglacial (i.e. incised on the
229 surfaces of the debris-covered glaciers). Consequently, it is reasonable to hypothesize
230 that these are glaciofluvial valleys. Although they date to the Amazonian Epoch and are
231 not ‘recent’ as defined in this review, these valleys attest to limited melting of the ice
232 contained in the debris-covered glaciers (Dickson et al., 2009; Fassett et al., 2010;
233 Howard and Moore, 2011) and are a part of a mid-latitude ice-related landscape
234 assemblage described below.

235

236 **3.5 *Pitted and scalloped terrains***

237

238 Scalloped depressions in mid-latitude regions (such as Utopia Planitia and Malea
239 Planum) display asymmetric cross sections in a north-south orientation, with pole-
240 facing scarps being steeper than equator-facing scarps. The depressions, which are

overprinted by polygonal patterns, are thought to be the result of the degradation of an ice-rich mantling deposit (e.g., Costard and Kargel, 1995; Lefort et al., 2009; Morgenstern et al., 2007; Zanetti et al., 2010). Although some studies suggested the presence of Amazonian-age thaw lakes inside the depressions (Costard and Kargel, 1995; Soare et al., 2007; Soare et al., 2008), the evidence for morphogenesis involving liquid water is ambiguous. The observed morphology can also be explained by dry degradation via sublimation (Séjourné et al., 2011; Ulrich et al., 2010). Numerical models of landform topographic profile development involving sublimation generate morphologies indistinguishable from profiles of actual topography rendered in HiRISE Digital Elevation Models (Lefort et al., 2009).

3.6 Pitted and fractured mounds

Some fractured mounds on Mars morphologically resemble terrestrial pingos. They occur both on plains such as Utopia Planitia and on the floors of impact craters and some recent (a few tens of million years at most; Burr et al., 2002b) flood-carved channels. Despite their morphological similarity, an origin as pingos is debatable. Other processes can result in similar morphologies (e.g., pseudocraters; Burr et al., 2009; Lanagan et al., 2001), and the mounds could also be erosional remnants of an ice-rich mantling (Dundas and McEwen, 2010; Hauber et al., 2011a). Mounds in Utopia

261 Planitia, however, might have formed as hydrostatic (closed-system) pingos on the
262 floors of possible thermokarst depressions, analogous to hydrostatic pingos on the floor
263 of drained thaw lakes on Earth (Burr et al., 2009). Alternatively, an origin of some
264 crater floor-mounds as hydraulic (open-system) pingos could also be envisaged. In this
265 scenario liquid water would be provided by basal melting of glaciers on the crater walls.
266 The water would then infiltrate the permafrost-free substrate beneath the glacier and
267 move downward and towards the crater floor, where it could build up artesian pressure
268 under the permafrost seal on the non-glaciated crater floor (Hauber et al., 2011a). Basal
269 melting on post-Noachian Mars would, however, require anomalously high heat flows
270 (Russell and Head, 2007) and it is highly unlikely that it would occur under recent
271 Martian environmental conditions (Fastook et al., 2012).

272

273 **3.7 Gullies**

274

275 Mid-latitude martian slopes are typically dissected by erosional features that resemble
276 ravines on Earth. As shown in Figure 3, they display a tripartite morphology, consisting
277 of an erosional alcove, one or several channels, and a depositional apron (Malin and
278 Edgett, 2000). The total lengths of these systems are commonly a few kilometres
279 (Balme et al., 2006). Despite these considerable dimensions, they were termed gullies
280 when first described in detail by Malin and Edgett (2000). Repeat observations revealed

current activity on some gullies (Diniaga et al., 2010; Dundas et al., 2010b; Reiss et al., 2010). Some of the changes, in particular the formation at two locations of bright deposits without apparent topographical changes (Malin et al., 2006) could be attributed to dry landsliding (Pelletier et al., 2008). Although several formational mechanisms were proposed, including flow suspended by liquid CO₂ (Musselwhite et al., 2001), dry granular flows (Treiman, 2003; Bart, 2007), and downwasting of accumulated CO₂ frost (Dundas et al., 2010b), there is a growing consensus that the overall morphology of gullies is best explained by processes involving liquid water, i.e. fluvial runoff or debris flows (e.g., Conway et al., 2011a; Mangold et al., 2010; Reiss et al., 2011). The gullies were originally suggested to have formed from seeps emerging from underground sources (Malin and Edgett, 2000), but the likely source of water is now thought to be melting of snow or near-surface ice (e.g., Williams et al., 2009; Balme et al., 2006; Costard et al., 2002; Dickson and Head, 2009; Levy et al., 2009b; Möhlmann, 2010).

3.8 Recurring slope lineae:

Repeat HiRISE images of southern hemisphere martian craters show the ongoing seasonal occurrence of dark slope lineae on some mid-latitude slopes in Mars' southern hemisphere (Figure 3; McEwen et al., 2011). These lineae recur in southern spring and summer predominantly on equator-facing scarps, where peak summer temperatures can

reach 250-300 K. Although several hypotheses regarding the origin of the slope lineae are discussed by McEwen et al. (2011), their favoured interpretation is the down slope transport of a salt-bearing, water-based liquid (e.g., a ‘cryobrine’ with a lowered freezing point; Möhlmann and Thomsen, 2011) that darkens the surface of the recurrent slope lineae through grain-wetting, and that then sublimates/evaporates once flow ceases after the summer thermal optimum. This mechanism is consistent with modelling of groundwater flow in sandy, unconsolidated regolith and is analogous to the formation of water tracks on slopes in Antarctica (Levy, 2012).

4. Landscapes on Mars indicative of thaw

Although all the landforms shown in table 1 probably formed in association with water-ice, not all require liquid water. Possibly the strongest evidence for liquid water from a single landform type comes from fluvial-like gullies (e.g., Conway et al., 2011a; Reiss et al., 2011). Nevertheless, inferring formative environments and processes from observations of individual landforms can be difficult, even on Earth and is more challenging on Mars, where the availability of in-situ field data of any kind is the exception, rather than the norm. Hence while synoptic studies of individual landforms such as gullies (e.g., Balme et al., 2006; Dickson et al., 2007), polygons (e.g., Levy et al., 2009a; Mangold, 2005) or glacial-like-forms (Souness et al., 2012) are important,

1
2
3
4
5
6
7
8
9 321 inferring process from form is challenging. Considering suites of landforms, and the
10 322 relationships between the individual elements, provides an alternative means of testing
11 323 hypotheses about morphogenesis. Hypotheses can be further tested by considering
12 324 whether on Mars the spatial and topographical distributions of a suite of landforms
13 325 within the landscape follow similar patterns to analogous landscapes on Earth (e.g.,
14 326 Balme and Gallagher, 2009; Levy et al., 2009b; Marchant and Head, 2007; Hauber et
15 327 al., 2011a). In the following sections, therefore,, we review three key landform
16 328 assemblages and the rationale used in the recent literature to infer component and
17 329 assemblage morphogenesis and environmental context, especially the spatially and
18 330 temporally varying geomorphic role of thaw liquids, on Mars in the recent past.. These
19 331 assemblages are dealt with here on a latitudinal basis to organise the literature but also
20 332 to emphasise the complex relationship between climate and landscape inheritance, for
21 333 example of topography, materials and volatiles, in morphogenesis.
22
23
24
25
26
27
28
29
30
31
32
33
34
35
36
37
38
39
40
41
42
43
44
45
46
47
48
49
50
51
52
53
54
55
56
57
58
59
60

335 ***4.1. Mid-latitude assemblage***

336
337 The mid-latitude regions of Mars, defined here as the areas between roughly 30° and
338 60° in both hemispheres, are particularly interesting for investigations of periglacial
339 processes for two main reasons. First, they represent an area of transition between the
340 high latitudes, which are characterized by a high amount of very near-surface ground ice

(e.g. Feldman et al., 2004), and the presently ice-free equatorial regions. Second, the mid-latitudes display a variety of landforms that are morphologically analogous to terrestrial periglacial surface features (e.g., Hauber et al., 2011b). Moreover, the distribution of many of these landforms is confined to the mid-latitudes, implying a climatic control. The mid-latitudes are also a region where ice is available as a prerequisite for melting, even if melting of such ice is probably a rare event (Costard et al., 2002; Hecht, 2002). Repeat remote sensing of fresh impact craters revealed that ground ice is present very close to the surface (Byrne et al., 2009), a view that was confirmed by spectral measurements showing evidence for water ice beneath CO₂ frost and an ice-free, rocky surface lag (Vincendon et al., 2010). Indeed, seasonal ice accumulation is an ongoing process in the mid-latitude regions, as repeat images demonstrate (Figure 4).

In the martian mid-latitudes there are at least two landscape types that host possibly periglacial features and which have morphological analogues on Earth. The first such landscape consists of plains without large-scale relief characterized by scalloped depressions that cut large polygons. In turn, the scalloped depressions are cross-cut by smaller polygons. Small mounds can be observed on the floors of some scalloped depressions and small craters. The northern parts of Utopia Planitia, in Mars' northern hemisphere provide a good example of this type of landscape. On Earth, similar

landform assemblages form in periglacial environments, the polygons being ice- or sand-wedge types, the depressions reflecting degradation of an ice-rich substrate and the mounds being hydrostatic (closed-system) pingos. Such landform assemblages are found in arctic lowland areas on Earth, e.g., in northern Siberia, which has been studied as a morphological analogue to Utopia Planitia on Mars (Ulrich et al., 2010). While the morphological evidence for ice in the near-surface is strong in this assemblage (Lefort et al., 2009; Morgenstern et al., 2007; Séjourné et al., 2011; Soare et al., 2005; Ulrich et al., 2011), the evidence for thaw is equivocal, for it is difficult to determine whether the scalloped depression formed by sublimation or melting.

The second broad type of periglacial landscape in the martian mid-latitudes is associated with large-scale topographic features such as impact craters, which provide considerable relief in both the heavily cratered southern highlands and the low-lying northern plains. Many craters host a series of landforms that could have a periglacial origin, including patterned grounds which are interpretable as possible ice-, sand-, or sublimation polygons, slope stripes, lobate landforms interpreted as debris-covered glaciers, gullies and slope lineae, and mound structures that are similar in shape and morphology to pingos. A morphologically analogous landscape is observed on Svalbard (Hauber et al., 2011b) where elements of both mountain (alpine) and lowland permafrost are present. The mountain massifs in Svalbard display slopes which are characterized by a variety of

381 sorting and permafrost creep processes (gelifluction, rock glaciers) as well as gullies
382 and debris-flow fans, while the floors of valleys exhibit widespread ice-wedge polygons
383 and many hydraulic (open-system) pingos.

384

385 An impact crater in the martian southern highlands (Fig. 6) provides an example of an
386 assemblage that is indicative of thaw, rather than just ice. The interior pole-facing crater
387 wall displays gullies, stripes, and creep features. The gullies and associated fans are
388 indicative of formation by fluvial and/or debris flow processes, both involving liquid
389 water. If the stripes formed by cryoturbation, their presence might indicate freeze/thaw
390 cycles. The slow creep of ice-rich permafrost material might have generated the lobate
391 features, but is not itself indicative of thaw.

392

393 A series of tentative scenarios that might explain the landform assemblages in mid-
394 latitude martian craters was suggested by Hauber et al. (2011a), ranging from prevailing
395 ‘wet’ processes (ice-wedge polygons, pingos) to a dominance of dry processes.
396 Importantly, however, all scenarios require at least some liquid water to explain the
397 occurrence of countless gullies on the inner and outer crater walls and the small fluvial
398 valleys down slope of the lobate (putative debris-covered glacier) features interpreted as
399 permafrost-related landforms.

400

401 *4.2 High-latitude assemblage*

402

403 There is extremely strong evidence from gamma ray and neutron spectroscopy that the
404 uppermost parts of the martian regolith at mid- to high-latitudes (ca. 60°N-75°N)
405 contain up to tens of weight-percents of water-ice (e.g., Boynton et al., 2002; Feldman
406 et al., 2004; Feldman et al., 2007). The evidence for liquid water in the mid-latitude
407 assemblage comes mainly from gullies and their association with other ice-related
408 landforms. At high latitudes, the evidence for water comes both from gullies and from a
409 variety of apparently sorted clastic landforms and their associations with one another
410 and the local topography. Martian periglacial sorted stripes and solifluction lobes were
411 inferred from MOC images by Mangold (2005) and in HiRISE images by Hauber et al.
412 (2011a), but in neither case could clasts be resolved. In contrast, Gallagher et al. (2011)
413 showed that slopes of many northern high-latitude impact craters of the order of 1-10
414 km diameter (e.g., Heimdal Crater near NASA's Phoenix Lander) are patterned by
415 clastic stripes, polygons, circles (Figure 7), possible solifluction lobes and terraces
416 (Figure 3d and Figure 8). What appear to be competent clasts, including ploughing
417 boulders (Johnsson et al., 2012) rather than puzzle rocks (Marchant and Head, 2007),
418 can be resolved in many of these features,. The landforms show a latitude-dependent
419 spatial distribution (Johnsson et al., 2011) and size-frequency statistics of superposed
420 impact craters (Gallagher et al., 2011) demonstrate that the crater retention age of the

421 surface is less than a few million years, and possibly even less than a few hundred
422 thousand years. On Earth, thaw is inherent to the sorting processes that create
423 periglacial assemblages like these, so thaw must also be considered as a possible
424 process for such landscapes on Mars. However, it should also be noted that there are
425 many more non-sorted polygonal fracture networks visible in these regions that could be
426 interpreted either as dry sand-wedge or sublimation-type polygons, and are probably not
427 indicative of wetter, ice-wedge polygons.

428

429 The textural distribution of clasts within the landforms and the morphology of the
430 landforms themselves is consistent throughout the region (Gallagher et al., 2011) and
431 accords with topographical context. For example, on Heimdal crater's rim, where
432 impact-exposed bedrock is closest to the surface, debris is largest and most abundant
433 (Figure 8). Exposed bedrock is relatively absent on the gentler outer crater walls and
434 available clasts tend to be smaller than in crater interiors (Figure 7b). Further from the
435 crater, sorted landforms are minimal and clasts even finer (Figure 7d), indicating that it
436 is possible that active layers are not present on low-slope surfaces (consistent with the
437 model of Kreslavsky, 2008). Clastic stripes occur on steeper slopes, more circular or
438 polygonal forms on less steep slopes (Figure 7), in agreement with terrestrial experience
439 (e.g., French, 2007) and formation models (e.g., Kessler and Werner, 2003). Throughout
440 the latitudinal zone of 60-75° N, the morphology of sorted forms associated with impact

craters is independent of background polygonal fracture networks that are also present here. Clasts are not concentrated within the fractures and some pristine fractures dissect clastic lobes, indicating that some fracturing post-dates sorting (Gallagher et al., 2011; Johnsson et al., 2012). Consequently, the systematic variation in landform morphology with slope and clast availability, and the cross-cutting relationship between fractures and sorted forms are not well explained by mechanisms relying on thermal contraction alone and not involving thaw and solifluction (e.g., Levy et al., 2008; Mellon et al., 2008).

The martian sorted clastic lobes are close morphological analogues of known solifluction lobes in Svalbard (Figure 2) and other terrestrial periglacial environments, with morphometric characteristics indicative of an origin involving thaw-generated solifluction rather than simply creep (Johnsson et al., 2011). For example, they are: planimetrically and dimensionally accordant; both populations originate at slope crests (Johnsson et al., 2012) or follow consecutively down slope from sorted clastic stripes at slope crests; down slope, the clasts in consecutive lobe chains become texturally finer (Ballantyne and Harris, 1994; Gallagher et al., 2011); both populations of lobes are characterised by arcuate, clast-banked overlapping risers (Johnsson et al., 2012).

Ground ice has been directly observed at the Mars Phoenix Lander Site, but only very minor regional thaw was modelled as being possible there by Mellon et al. (2008) prior to the landing of Phoenix. Because the modelled amount of thaw fluid was deemed insufficient to be geomorphically effective, Mellon et al. (2008) and Levy et al. (2010) explained sorting to be a consequence of clast collapse into thermal contraction cracks in a dry environment characterized by sublimation, not thaw. However, sorted clastic mounds, nets, polygons and stripes are landforms widely associated on Earth with freeze-thaw cryoturbation (e.g., Kessler and Werner, 2003) and, as already described, neither the morphology nor the plan form organization of the martian sorted clastic landforms is accordant with underlying fracture patterns. Accordingly, periglacial freeze-thaw sorting offers a plausible explanation of the martian high-latitude morphological assemblage, including its spatial and clinometric contexts and the inter-relationships of its components.

Importantly, fluvial gullies are intimately tied to both sorted and non-sorted landforms in this region (e.g. Figure 9). Of the braided gullies identified, some predate, and others post-date ground patterned by cracks, polygons, circles and lobes (Gallagher and Balme, 2011; Gallagher et al., 2011). Once again, these landforms on Mars have a close analogue on Svalbard, where sorted lobes and patterned ground are spatially correlated with braided gullies and thermal contraction fractures (Johnsson et al., 2011). Levy et

al. (2009b) described gully-polygon interaction in the Dry Valleys of Antarctica that are also analogous to martian gully polygon associations, and they suggested a genetic link between martian gullies and periglacial/permafrost landform assemblages, including polygonally patterned ground (Levy et al., 2009a).

Gully erosion all the way back to the crater rim (e.g., Figure 9) suggests that these fluvatile systems (for a discussion of the characteristics of debris flow versus “fluvial” gullies on Mars see Reiss et al., 2011) are the product of incision by thaw fluids seeping from solifluction lobes, from frost melt or even from snow melt trapped in polygonal fracture networks (Levy et al., 2009b). However, other explanations such as rim flattening by creep and mass wasting, and extensive loss of crater-rim ground-ice reservoirs, cannot be excluded. Hence, from the co-association of these landforms, Gallagher et al. (2011), Gallagher and Balme (2011) and Johnsson, et al. (2011) inferred the widespread action of freeze-thaw in a fluvio-periglacial context.

In summary, lobate clastic and non-clastic features are close analogues of solifluction lobes on Earth. The association in time and space of apparent solifluction landforms and sorted stone stripes, circles and polygons with gullies suggests that there was at least enough liquid available for gully formation, although obtaining quantitative estimates of thaw rate or the volume of thaw liquid from morphology alone is difficult and only first-

order estimates can be made (Gallagher and Balme, 2011). Similarly, the association with polygonal fractures of probable thermal-contraction origin provide consistent evidence for ice in the regolith, and could be taken as evidence for a change in climate from wetter conditions when the solifluction lobes formed, to dryer when thermal contraction and sublimation dominated.

4.3. Equatorial Assemblage

This assemblage, described more fully in Balme and Gallagher (2009), is distinct from those previously discussed in that i) it pertains to a single locale at the head of the outflow channel ‘Athabasca Valles’, rather than a latitude range and ii) the proposed source of ice in the regolith was almost certainly fluvial floodwaters, rather than atmospheric precipitation or condensation. The evidence for thaw includes polygonally patterned surfaces hosting landforms analogous to retrogressive thaw slumps (RTS); merged basins (containing RTS and secondary polygonal patterned ground) that evolved through downwearing and backwearing; pingo-like cones and mounds within these basins; and apparent slope subsidence failures. The interpretation is that this assemblage of landforms reflects a relict thermokarst landscape that formed in icy sediments left behind after megaflooding, but it seems unlikely that such thaw-related processes are ongoing today.

1
2
3
4
5
6
7
8
9 520

10 521 This study area at the head of Athabasca Valles is near the equator (~10.2° N 157° E)
11
12 522 and represents the source regions of a flood-carved outflow channel (Burr et al., 2002a;
13
14 523 Burr et al., 2002b) that begins at a large fracture system called the Cerberus Fossae
15
16 524 (Figure 10) and which is thought to be the source of the flood waters. The Athabasca
17
18 525 Valles source region comprises two amphitheatre-shaped depressions which open to the
19
20 526 southwest. These two depressions merge to form the main channel, which slopes away
21
22 527 from the source region with a gradient of approximately 0.3° and a slightly concave
23
24 528 long profile. The proximal five to ten kilometres of the channel slope back towards the
25
26 529 source region and it is within this shallow basin that landforms interpreted to be
27
28 530 indicative of thaw have been identified (Balme and Gallagher, 2009).
29
30
31
32

33 531

34
35 532 The basin floor south of the southern Cerberus Fossae fracture comprises a series of
36
37 533 polygonally-patterned surfaces (Figure 11) and shallow basins. The surfaces are
38
39 534 separated by distinctive scarps (Figure 11) indented by cirque-shaped indentations or
40
41 535 niches, and broad, v-shaped 'bays'. In Figure 11, scarp formation has apparently been
42
43 536 by retrogressive erosion (cf. 'backwearing', Czudek and Demek, 1970) into the
44
45 537 polygonised surface, accompanied by the contemporaneous (or immediately
46
47 538 subsequent) release of debris and the stranding of large (meter-scale) clasts by the
48
49 539 formation of dendritic channels at the base of the scarps. Remnant spurs appear to
50
51
52
53
54
55
56
57
58
59
60

1
2
3
4
5
6
7
8
9
10
11
12
13
14
15
16
17
18
19
20
21
22
23
24
25
26
27
28
29
30
31
32
33
34
35
36
37
38
39
40
41
42
43
44
45
46
47
48
49
50
51
52
53
54
55
56
57
58
59
60

540 demonstrate the minimum original extent of the upper surface prior to backwearing,
541 which, given the size and shape of the smallest embayments, might have exploited the
542 polygonised pattern of the upper surface (Balme and Gallagher, 2009).

543

544 The channels have a contributory form and, as shown in Figure 11, at least one example
545 terminates at the margins of a shallow depression with a distinctive hummocky floor.
546 Possible lobate flows with subtle leveed channels can be seen in this example.
547 Hummocky material with similar morphology occurs at the terminations of other
548 channel systems in this region. Balme and Gallagher (2009) suggest that these forms are
549 analogous to terrestrial retrogressive thaw slumps (RTS): landforms that on Earth are
550 diagnostic of degrading ice-rich permafrost (Harris, 1981).

551

552 Nearby, similar niche and spur scarp morphologies form the boundaries of linked basins
553 (Figure 12). Importantly, polygonally patterned ground occurs on the sloping inner
554 walls of these basins, beneath the niche-indented headwalls of the basin margins. If the
555 scarps formed by retrogressive erosion, then this polygonization must be secondary in
556 origin, and have formed after or as the backwearing occurred. Small gullies can be seen
557 on the inner slopes of these basins, again suggesting fluvial erosion. The floors of these
558 linked basins are hummocky and rough and contain small pitted-cone or pitted-mounds.
559 These linked basins speak of significant downwearing and backwearing of enlarging

1
2
3
4
5
6
7
8
9 560 depressions, with some examples showing small outflow channels (e.g. at Z in Figure
10
11 561 12) which points to flow of fluid through ‘tapping’ (Hill and Solomon, 1999) channels
12
13 562 as the basins expanded and merged. The evolutionary pattern of these linked basins and
14
15 563 scarp systems implies liberation of a volatile from within the regolith. This volatile was
16
17 564 probably water, given the regional flood-channel setting and the small gullies and
18
19 565 fluvial-like channels seen here. If this is the case, these basins probably represent
20
21 566 thermokarst depressions, and the mound and cone landforms are likely to be remnant
22
23 567 pingos.
24
25
26 568

27
28 569 A nearby closed, shallow basin within the main Athabasca Channel (Figure 13) is
29
30 570 surrounded by polygonal terrain and internally partitioned by low causeways of domed
31
32 571 polygons or niche-indented headlands. Many of the niches, especially on the western
33
34 572 margin of the basin, are fronted by scarp-parallel ridges that appear to have been formed
35
36 573 by subsidence failures. The composite form of the basin suggests that it evolved from a
37
38 574 series of smaller basins that became linked as they enlarged and merged. The basin
39
40 575 contains groups of cone and mound landforms that are spatially associated with either
41
42 576 the lowest points of the basin floor, or with channels feeding (or perhaps draining) the
43
44 577 basin (e.g. Y, Figure 13). This association is consistent with a tapping model (Hill and
45
46 578 Solomon, 1999) of basin evolution wherein fluid filled basins grow and merge with
47
48 579 liquid transferring between them by small channels. The cone and mound landforms
49
50
51
52
53
54
55
56
57
58
59
60

1
2
3
4
5
6
7
8
9
10
11
12
13
14
15
16
17
18
19
20
21
22
23
24
25
26
27
28
29
30
31
32
33
34
35
36
37
38
39
40
41
42
43
44
45
46
47
48
49
50
51
52
53
54
55
56
57
58
59
60

580 display a range of morphologies, from simple mounds, through pitted cones, to cone
581 groups situated within ramparts and moats. Some of the cone/mounds, especially in the
582 southeast, appear degraded. Again, if the basin formed by thermokarst, these features
583 are probably pingos, as has been suggested for other regions of Athabasca Valles (Burr
584 et al., 2005; Page and Murray, 2006).

585

586 To summarise: 1) locally high, planar surfaces are modified by planar and domed
587 polygons, 2) these surfaces are truncated by cirque-shaped scarps probably formed by
588 failures along polygon edges, 3) the scarps are fronted by inclined slumps and flows
589 modified again by domed polygons, 4) the slumps and flows are often incised by
590 channels and gullies and often terminate at a break of slope marking the margin of 5) a
591 hummocky, debris-floored basin, containing cone/mound landforms, 6) in gently
592 sloping regions, these processes form linear scarps perpendicular to slopes; in flatter
593 areas, autogenic basin formation and enlargement leads to complex topography.

594

595 Given both the consistent similarity between this assemblage and thermokarst
596 landscapes on Earth, and the regional context of a flood-carved channel, the most likely
597 explanation of these observations appears to be a linked mass wasting environment
598 controlled by the thaw of ground ice in the locally uppermost surfaces. Subsidence has
599 destroyed the original surface relief but new thermokarst relief has formed at a lower

1
2
3
4
5
6
7
8
9 600 elevation by both downwearing and backwearing (Czudek and Demek, 1970; French,
10 601 2007) The result is a landscape of self-similar elements reflecting multiple cycles of
11
12 602 surface reworking by a single set of processes in which thaw plays a key role.
13
14
15 603

16 17 604 **5. Discussion**

18
19
20 605

21 606 ***5.1 Terrestrial analogues***

22
23
24 607

25
26 608 In each of the three assemblages described, terrestrial analogues have been vital in
27
28 609 understanding the landscape. While the use of terrestrial analogues is essential in any
29
30 610 analysis of the martian landscape, it is also critical to recognize the limits of this
31
32 611 approach, as vegetation (or lack thereof), mineralogy, rock type and landscape
33
34 612 evolution, including the role of transitions between landscape convergence and
35
36 613 divergence should all be taken into account but are often impossible to characterise with
37
38 614 any certainty, let alone quantify. For example, the landscape of Svalbard provides very
39
40 615 good morphological analogues of Mars, but its climatic conditions are significantly
41
42 616 different from present martian conditions, and also different from what can reasonably
43
44 617 be expected to have existed on Mars over the last few million years. Mars is, compared
45
46 618 with terrestrial standards, exceptionally cold and dry, and from that viewpoint Svalbard
47
48
49 619 could be regarded as a poor climatic analogue, despite the landform assemblages it
50
51
52
53
54
55
56
57
58
59
60

620 shares with Mars, such as those including patterned ground, sorted mass wasting slope
621 deposits and gullies. Hyperarid cold deserts such as those found in places of the
622 Canadian High Arctic, Greenland, or particularly in continental Antarctica may provide
623 climatic conditions that are closer to those prevailing on Mars. Indeed the McMurdo
624 Dry Valleys of Antarctica have a long history as analogues for different aspects of Mars
625 studies (e.g., Chapman, 2007; Doran et al., 2010; Marchant and Head, 2007) and an
626 interpretation of some martian landforms based on the hyperarid polar desert analogue
627 yields very plausible results, as in the case of Antarctic sand-wedge polygons. However,
628 not all features (e.g., slope stripes and solifluction lobes) observed on Mars have
629 analogues in the coldest, driest regions of terrestrial cold deserts (e.g., the 'stable upland
630 zone' of the Antarctic Dry Valleys described by Marchant and Head, 2007) that are most
631 Mars-like in climate. So, there is probably no single analogue landscape on Earth that
632 can serve to explain all the observed characteristics of martian landscape. However,
633 terrestrial landscapes still provide vital analogues, as they demonstrate how landscapes
634 are shaped by different processes and involve variable degrees of morphological
635 inheritance from earlier process environments. Hence, it is important to note that there
636 are regions on Earth that are good process analogues, and others that are good climate
637 analogues (and some areas that are both) as well as recognizing that while morphology
638 can sometimes be process-specific, processes are not generally climatically specific, so
639 linking morphology directly to climate in an absolute sense is extremely challenging.

640

641 ***5.2 Evidence for thaw***

642 In the mid-latitudes on Mars, the presence of a suite of landforms associated with ice
643 strengthens the arguments that both gullies and pro- and supraglacial valleys were
644 formed by melt of ice to form liquid water. Without the presence of landforms
645 indicative of ice, it would be difficult to imagine how liquid water could be generated,
646 unless by seepage or outburst from underground (and this has been shown to be
647 unlikely, at least for gullies; Balme et al., 2006; Dickson and Head, 2009; Reiss et al.,
648 2009). By way of confirmation that martian gullies were not formed by dry processes,
649 Conway et al. (2011a) used morphometric terrain analysis techniques to show that
650 martian gullies are more similar to 'wet' terrestrial debris flow chutes than they are to
651 dry, colluvial fans. This approach provides a way around the problem of equifinality
652 brought up by Bart (2007), who suggested gullies on the Moon (presumably formed by
653 water-free processes) are morphologically similar to gullies on Mars. However, such
654 techniques are not universally applicable, for they require very high spatial resolution
655 topographic data that are available only for a few areas of Mars, and are restricted to
656 certain classes of hillslope landform. Nevertheless, as more high fidelity topographic
657 data are returned from Mars and other planets, such quantitative techniques could
658 provide an additional way to infer process from form.

659

660 Similarly, the solifluction lobes and sorted patterned ground seen at high latitudes are
661 themselves strong evidence for the presence of freeze-thaw cycles, but the key
662 observation supporting this interpretation is their spatial and temporal associations with
663 gullies (indicating liquid water flow) and a variety of polygonally patterned ground
664 (indicating the presence of water-ice). The simplest interpretation of this landscape is
665 that there was water-ice within and/or covering the regolith and that, at some point in
666 the recent past, thaw of ice or snow led to sufficiently intense incision (perhaps
667 generated only by rare short-lived events) to form the gullies, the sorted landforms
668 having been formed by freeze-thaw processes within the regolith. This hypothesis is
669 consistent with all the local geomorphology. Conversely, hypotheses for formation of
670 sorted ground in this region based solely on dry processes seem unlikely (e.g., Orloff et
671 al., 2012; Orloff et al., 2011), as they explain neither the gullies nor the lobate forms. It
672 is likely that most of the high latitude patterned ground seen on Mars did not form by
673 thaw-related processes (Levy et al., 2009a; Mellon et al., 2008), particularly across the
674 extensive, flat plains regions in the northern martian lowlands, but this does not mean
675 that thaw, as described here, was not a geomorphic agent in numerous high latitude
676 local examples.

677

678 The low latitude assemblage described at the head of Athabasca Valles appears to be
679 best explained by thaw of ice-rich flood deposits. This landscape probably formed out

of equilibrium with the climate, unlike the other assemblages where both deposition and removal of ice has likely been climate controlled, for its characteristic morphologies and their spatial organisation are determined by the spatial pattern and morphology of surface floodwater storage sinks and deposits. Certainly, there is no evidence for ice or thaw related landforms immediately outside of the putatively flood-related terrain. In some ways, the presence of thaw here is not unexpected. The sudden deposition of massive amounts of ice, water and debris onto the surface in a region near Mars' equator would have meant that conditions for thaw would be optimum in terms of temperature. However, it should be noted that these same polygonally patterned ground have been interpreted by some researchers (e.g., Jaeger et al., 2010; Keszthelyi et al., 2000; Keszthelyi et al., 2004; Plescia, 1990; Ryan and Christensen, 2012) to be primary extrusive volcanic deposits, rather than the expression of secondary modification of ice-rich flood sediments (e.g., Balme and Gallagher, 2009; Burr et al., 2005; Page, 2007), although no volcanic interpretation has yet been advanced that explains all the landforms and their spatial association in this specific location in the same way that the thermokarst hypothesis does. Both interpretations might be correct to some extent, for the periglacial assemblage could have developed within or on top of primary volcanic material after the water ice and sediments were brought in following flooding.

699 The geologically recent thaw-modified landscapes described here are distributed around
700 the globe, and at low to high latitudes. Those landscapes including features such as
701 stone circles, stripes and solifluction-like lobes are perhaps indicative not only of
702 surface melt, but also of ground ice thawing cycles. Similarly, observations and surveys
703 of populations of gullies provide evidence for surface thaw (at least for those gullies
704 found on polygonised substrates; Levy et al., 2009b) from mid to high latitudes in both
705 hemispheres (e.g. Balme et al., 2006; Kneissl et al., 2009; Malin and Edgett, 2000).
706 Hence geologically recent thaw appears to be fairly common on Mars. Nevertheless,
707 compared with other morphological indicators of ice (but not thaw) such as polygonally
708 patterned grounds interpreted to be thermal contraction fractures (e.g., Levy et al.,
709 2009a; Mangold, 2005; Mellon, 1997) the distribution of thaw related landforms is
710 spatially very restricted. Hence, thaw is not likely to have been a globally dominant
711 process in the recent past, but as the examples shown above demonstrate, local
712 examples of thaw can be found globally.

713

714 ***5.3 Hypotheses to explain thaw***

715

716 One broad interpretation of the martian geomorphology described in this paper is that
717 both fluid flow and freeze-thaw cycles have, to some extent, shaped the surface
718 throughout the mid- and high-latitudes in the recent past, and that these processes have

1
2
3
4
5
6
7
8
9 719 even occurred in specific process environments near the equator. However, given the
10
11 720 inhospitality of the current martian environment to liquid water, this leads to an
12
13 721 apparent paradox – the landscape appears to be shaped by liquid water, but thaw of ice
14
15 722 to produce liquid water under today's cold and dry climate is not predicted in general
16
17 723 (Ingersoll, 1970). This is because near-surface ground ice on Mars sublimates in the low
18
19 724 humidity conditions, except nearer the poles where the temperatures are colder and
20
21 725 hence the saturation point and sublimation rate lower. Hence to melt, ice must either be
22
23 726 warmed sufficiently quickly for sublimation cooling to be offset, or diffusion of water
24
25 727 vapour from the ice must be minimized such that sublimation is restricted. These criteria
26
27 728 can be met only under specific conditions such as coating by dust, overlying and
28
29 729 removal of CO₂ ice, or the presence of salts, (see, for example, the summary section of
30
31 730 Hecht, 2002). It should also be noted, though, that surface liquid water can remain in
32
33 731 disequilibrium long enough to do significant geomorphic work and flow significant
34
35 732 distances if it can be produced quickly enough (e.g., Heldmann et al., 2005; Conway et
36
37 733 al., 2011b) even under present day conditions.
38
39
40
41
42
43

44 735 A first possible solution to this paradox is that brines with low freezing points
45
46 736 (cryobrines) are the active geomorphological agents rather than pure water. Some brines
47
48 737 can remain liquid at temperatures tens of degrees colder than the freezing point of pure
49
50 738 water (e.g., Knauth and Burt, 2002; Möhlmann and Thomsen, 2011). The detection of
51
52
53
54
55
56
57
58
59
60

perchlorate at the Phoenix landing site (Hecht et al., 2009) has provided observational evidence for salts on Mars that have a low eutectic temperature and might allow for the possibility of liquid brines today (e.g., Marion et al., 2009). Magnesium, calcium and sodium are possible anion pairs (Hecht et al., 2009) and their perchlorates all have eutectic temperatures below 240 K (Marion et al., 2009; Pestova et al., 2005). Interestingly, the eutectic temperature of magnesium perchlorate is within the range of spring/summer diurnal variations modelled and measured for the Phoenix Landing Site (Zent et al., 2010). The most recently discovered ‘wet’ landforms – recurring slope lineae (McEwen et al., 2011) – are forming on Mars at the present time, most likely associated with active, but spatially uncommon, flows of cryobrines at low temperatures and in a thin, dry atmosphere

A second solution to the apparent paradox is the possibility that those landforms attributed to thaw processes (e.g. gullies, sorted stripes and circles, clastic lobes) are a climatically controlled assemblage, reflecting significantly warmer conditions than those prevailing now. This hypothesis maintains that it was melt of water-ice to form liquid water at ~273 K that shaped the landscape, rather than the action of cryobrines acting under a climate similar to the present-day. For example, Kreslavsky et al. (2008) calculate that an active layer (i.e. near-surface temperatures consistently above 273K) can develop on Mars due to changes in the climate driven by ~ 120 ka cycles in

1
2
3
4
5
6
7
8
9 759 obliquity. Such conditions might allow thaw in suitable microclimates, even if the
10 760 global climate was unsuited to regional melt of water ice. Similar mechanisms have
11
12 761 been proposed to explain the formation of gullies on Mars (e.g., Christensen, 2003;
13
14 762 Costard et al., 2002; Dickson and Head, 2009; Levy et al., 2009b; Williams et al.,
15
16 763 2009). In contrast, though, the present activity of recurring slope lineae seems to show
17
18 764 liquid-based activity under present day conditions, although it should be noted that at
19
20 765 the time of writing, recurring slope lineae have been found in very few locations
21
22 766 compared with gullies or other putative thaw-related landforms. Also, the presence of a
23
24 767 relict thermokarst assemblage near the martian equator demonstrates that local-to-
25
26 768 regional inheritance of form and materials can play a crucial role in modulating
27
28 769 morphogenetic responses to prevailing climate.
29
30
31
32

33 770

34
35 771 The small size and lack of degradation of many of the landforms and landscapes
36
37 772 described here mean that it is difficult to determine their age based on the size
38
39 773 frequency statistics of superposed impact craters or erosion rate estimates, so it is
40
41 774 extremely challenging to determine whether any given landform formed under current
42
43 775 or recent past climatic conditions, unless that landform can be observed to change. In
44
45 776 addition, the two hypotheses proposed are not exclusive, and perhaps both were valid at
46
47 777 different locations and times.
48
49

50 778
51
52
53
54
55
56
57
58
59
60

779 **5.4 Can these hypotheses be tested?**

780

781 The first hypothesis is difficult to test without in-situ studies to confirm the chemical
782 composition of, for example, deposits or surfaces associated with thaw-related
783 landforms. Hyperspectral remote sensing studies (e.g., Murchie and the CRISM Science
784 Team, 2007) might also be used by measuring the reflectance spectra of minerals in the
785 regions where, for example, recurring slope lineae are forming. Current instruments
786 probably lack the spatial resolution for this task, however: initial studies of the recurring
787 slope lineae McEwen et al. (2011) find that hydrated minerals are associated with
788 bedrock at several sites where recurring slope lineae have formed (including
789 phyllosilicates in Asimov Crater and chlorite, kaolinite, and hydrated silica in the
790 central structure of Horowitz Crater) but they do not find a correlation between
791 recurring slope lineae regions and particular minerals. Laboratory studies aimed at
792 testing whether phase changes in hydrated minerals can perform the same
793 geomorphological work that freeze-thaw of ice does could also be used to, at the least,
794 demonstrate that the hypothesis is plausible.

795

796 The second hypothesis has been investigated in some detail, and more work is
797 underway. For example, Kreslavsky et al. (2008) used a model of Mars' past obliquity
798 and eccentricity (from Laskar et al., 2004) to calculate spatial variations in peak

insolation over the past few million years on Mars. They found that seasonal thaw waves (>273 K) penetrating to tens of centimetres depths could have occurred in several periods during the last 20 Ma. Kreslavsky et al. (2008) also found that local slope, albedo, and regolith properties play a significant role in determining the depth of such an active layer. They note also that active layer formation is rather rare, and that it is only on steep slopes at high latitudes, during high obliquity periods, that an active layer might develop (cf. section 4.3 above). Whether liquid water could form from segregation ice or pore ice and then remain stable against boiling and evaporation within the regolith long enough to do significant geomorphological work is unknown, and would depend mainly on the properties of the regolith and the rate at which water-vapour would diffuse from it (Hudson et al., 2007). Furthermore, Möhlmann (2010) suggests that the 'solid-state greenhouse effect' allows insolation energy to be absorbed within snow or ice packs, allowing internal ice or snow to heat up and perhaps even melt, while the upper surface remains at sub-freezing temperatures. He calculates that melt of snow or ice is possible under present-day condition on Mars, at least for some regions and deposits. This mechanism might be important for generating melt within the source regions of gullies, although it is less relevant to the melting of ground-ice and the formation of patterned ground.

5.5 Implications of thaw

819

820 The formation of liquid water on Mars seems possible, but requires special
821 circumstance – either the presence of optically thin snow and ice deposits to create a
822 solid-state greenhouse, climate change in the recent past, or the presence of salts that
823 can depress the freezing point of the water. If it can be determined which (if any) of
824 these process-suites were responsible for creating the thaw-related landscapes described
825 here, this raises the question as to whether geomorphological observations can be used
826 to provide information about past environment on Mars. Of course, inferring
827 environment from landform is difficult, even on Earth. Current landscapes can still
828 display an imprint of former climatic conditions (e.g., André, 2003; French, 2007;
829 Twidale, 1999) so disentangling signals from remote sensing alone is a challenge. Also,
830 as has been demonstrated for the Earth (e.g., Matsuoka, 2011; Murton and Kolstrup,
831 2003), it is unlikely that any single landform can be used as a quantitative indicator of
832 past and/or present climatic conditions. Nevertheless, as the martian landscape is a
833 simpler system than on Earth, with no plate tectonics, no vegetation, less water, and
834 lower erosion rates, it is possible that the link between climate and landforms on Mars
835 could be more direct.

836

837 In summary, although the morphological signatures of thaw are now becoming better-
838 recognized, a lot of work remains to be done if these observations are to be placed into a

839 consistent framework explaining how Mars' surface and climate have evolved in the
840 past few million years.

841

842 **6. Ongoing and future directions for research**

843

844 Identification of many of the landforms described here has only been possible since
845 HiRISE images with sub-meter resolution became available in 2006. Hence, this branch
846 of martian geomorphology is advancing particularly quickly. For example, while
847 decametre-scale patterned ground at high-latitude on Mars has been well documented
848 for over a decade (e.g., Levy et al., 2009a; Levy et al., 2010; Mangold, 2005; Mellon,
849 1997; Seibert and Kargel, 2001) and all of these authors considered thaw as a
850 geomorphic process in polygon formation, it has largely been rejected on the weight of
851 the evidence. Yet in the past two years, solifluction-like landforms within these regions
852 have been described in four papers (Gallagher et al., 2011; Gallagher and Balme, 2011;
853 Hauber et al., 2011a; Johnsson et al., 2011). HiRISE images cover less than a few
854 percent of the surface, and more images are being acquired daily, so most of Mars
855 remains unexplored at this scale and the study of possible solifluction lobes and sorted
856 patterned ground on Mars is still, therefore, rather in its infancy. To help constrain how
857 such landscapes evolved, and under what climate conditions, a primary data set
858 describing both the global distribution of such landforms, and their regional-scale

1
2
3
4
5
6
7
8
9
10
11
12
13
14
15
16
17
18
19
20
21
22
23
24
25
26
27
28
29
30
31
32
33
34
35
36
37
38
39
40
41
42
43
44
45
46
47
48
49
50
51
52
53
54
55
56
57
58
59
60

859 geological context is needed. Such work might also explain the observations that, in the
860 high- and mid-latitudes, many of the landforms indicative of thaw, such as gullies,
861 sorted stripes and solifluction lobe-like features, occur on steep slopes. This is
862 consistent with models of martian active layer formation (Kreslavsky et al., 2008) on
863 Mars, and liquid water stability (Hecht, 2002). Interestingly, the low latitude
864 assemblage described is in a flat region, but has a different suite of landforms. Hence, it
865 would be informative to compare the different morphologies and assemblages with high
866 resolution terrain models as well as to regional and local climate models.

867

868 While some landforms such as recurring slope lineae are forming today, perhaps most
869 landforms indicative of freeze/thaw did not form on present-day Mars, but during
870 periods with different climates. To test this hypothesis, a much better understanding of
871 the martian climate in the last ~20 Ma as a function of obliquity and other orbital
872 parameters is required. Such information would help to constrain precipitation patterns,
873 the frequency of freeze/thaw cycles and the associated amount of liquid water available
874 (if any). Advances in assessment of past environmental conditions will come from
875 climate modelling at different scales (including meso-scale models and the analysis of
876 local relief-dependent microclimates).

877

878 As described in section 5.3, some hydrated minerals have the capacity to capture, store,
879 and release large amounts of water from their chemical structures at temperatures well
880 below 273 K. Hence these processes could be important on cold Mars, playing the same
881 geomorphic role the water-ice transition does in periglacial regions on Earth. However,
882 not enough is known about the behaviour of these materials under martian conditions to
883 verify whether they can play such a role in shaping the surface. Laboratory investigation
884 of their behaviour as a function of past and present martian temperature, regolith-cover,
885 and interaction with ground ice is needed. A particularly important early study could be
886 to simulate the conditions at which the recurring slope lineae (McEwen et al., 2011)
887 formed, in order to investigate whether salt/regolith/ice mixtures could generate liquids
888 as seasonal conditions change as suggested (McEwen et al., 2011).

890 Although periglacial landforms have been observed on Mars and are thought to be
891 'young' due to the lack of superposing impact craters, the rates at which periglacial
892 processes operate on Mars, inferred from these morphologies, are unknown. It might be
893 envisaged that they operate orders of magnitudes slower than on Earth, for liquid water
894 is probably available only episodically, in small amounts, and in spatially and/or
895 temporally restricted circumstances. Coupled with Mars' low erosion rates, this would
896 perhaps offer an explanation why we observe apparently young periglacial landforms on
897 Mars: the same process might shape a landform very quickly on Earth (e.g., on post-

898 glacial surfaces in the Holocene, within thousands of years) if substantial amounts of
899 liquid water are available, but could require hundreds of thousands or even millions of
900 years to form an analogous landform under current martian conditions. Dating martian
901 periglacial surfaces and landforms by the statistical analysis of the numbers of very
902 small impact craters superposing them would be a challenging (especially given the
903 ongoing controversy surrounding the use of small crater counts as a dating tool; e.g.,
904 Hartmann, 2007; McEwen and Bierhaus, 2006), but productive, future area for research
905
906 More field studies are needed to help understand terrestrial landscapes as periglacial
907 process-analogues for Mars, and to understand how climate controls or modifies these
908 processes. This is, of course, a broad question, but the contrasting hyperarid polar desert
909 climate of the Dry Valleys in Antarctica and the periglacial cold and relatively moist
910 (although still close to polar desert conditions) climate of Svalbard provide a good
911 starting point for Mars research. Both locations provide suites of periglacial landforms
912 that are good process and morphological analogues for Mars, yet the details of the
913 assemblages are different. Interestingly, certain martian regions (especially at high
914 latitude) contain landforms directly analogous to examples from both Svalbard and
915 Antarctica. Hence, it would be instructive to learn more about when, how fast, and
916 under what climatic conditions the terrestrial landforms were created, for this could
917 provide important constraints on the environments under which the martian landforms

918 were formed, and how the landscape evolved as – presumably – climate changes
919 occurred.

920

921 Finally, an underlying methodological aspiration vital for this type of research is to find
922 a way to determine how much meltwater is involved in martian landscape development.
923 Such an approach could help discriminate between wet versus dry morphogenesis, and
924 even between surface melt (of ice or snow) and subsurface melt (i.e. active layer
925 formation). Connecting the extent of thaw needed to form the various landforms to the
926 overall landscape thaw generation potential could be a very valuable way of recasting
927 and testing the climate implications of various landscape analyses. Attempts to follow
928 such a methodology using both qualitative (e.g., Hauber et al., 2011a) and quantitative
929 terrain analyses (e.g., Conway et al., 2011a) are already making progress.

930

931 6. References

- 932 Aharonson O and Schorghofer N. (2007) Subsurface ice on Mars with rough
933 topography. *J. Geophys. Res.* 111: doi:10.1029/2005JE002636
934 Albee AL, Arvidson RE, Palluconi F, et al. (2001) Overview of the Mars Global
935 Surveyor mission. *J. Geophys. Res.* 106: 23,291-223,316.
936 André, M-F. (2003) Do periglacial landscapes evolve under periglacial conditions?
937 *Geomorphology* 52: 149-164.
938 Ansan V and Mangold N. (2006) New observations of Warrego Valles, Mars: evidence
939 for precipitation and surface runoff. *Plan. Space Sci.* 54: 219-242.
940 Baker VR. (2001) Water and the martian landscape. *Nature* 412: 228-236.
941 Baker VR, Strom RG, Gulick VC, et al. (1991) Ancient oceans, ice sheets, and the
942 hydrological cycle on Mars. *Nature* 352: 589-594.

943 Ballantyne CK and Harris C. (1994) *The periglaciation of Great Britain*, Cambridge:
944 Cambridge University Press.

945 Balme MR and Gallagher C. (2009) An equatorial periglacial landscape on Mars. *Earth*
946 *Planet. Sci. Let.* 285: 1-15.

947 Balme MR, Gallagher C, Page DP, et al. (2009) Sorted stone circles in Elysium Planitia,
948 Mars: implications for recent martian climate. *Icarus* 200: 30-38.

949 Balme MR, Mangold N, Baratoux D, et al. (2006) Orientation and distribution of recent
950 gullies in the southern hemisphere of Mars: observations from HRSC/MEX and
951 MOC/MGS data. *J. Geophys. Res.*: E05001, doi: 05010.01029/02005JE002607.

952 Bargery AS, Balme MR, Warner N, et al. (2011) A background to Mars exploration and
953 research. In: Balme MR, Bargery AS, Gallagher CJ, et al. (eds) *Martian*
954 *Geomorphology*. London: Geological Society., 5-20.

955 Bart G. (2007) Comparison of small lunar landslides and martian gullies. *Icarus* 187:
956 417-421.

957 Berthling I. (2011) Beyond confusion: Rock glaciers as cryo-conditioned landforms.
958 *Geomorphology* 131: 98-106.

959 Boynton WV, Feldman WC, Squyres SW, et al. (2002) Distribution of hydrogen in the
960 near surface of Mars: Evidence for subsurface ice deposits. *Science* 297: 81-85.

961 Burr DM, Grier JA, McEwen AS, et al. (2002a) Repeated Aqueous Flooding from the
962 Cerberus Fossae: Evidence for Very Recently Extant, Deep Groundwater on
963 Mars. *Icarus* 159: 53-73.

964 Burr DM, McEwen AS and Sakimoto SEH. (2002b) Recent aqueous floods from the
965 Cerberus Fossae, Mars. *Geophysical Research Letters* 29:
966 doi:10.1029/2001GL013345.

967 Burr DM, Soare RJ, Wan Bun Tseung, J-M, et al. (2005) Young (late Amazonian),
968 near-surface, ground ice features near the equator, Athabasca Valles, Mars.
969 *Icarus* 178: 56-73.

970 Burr DM, Tanaka KL and Yoshikawa K. (2009) Pingos on Earth and Mars. *Plan. Space*
971 *Sci.* 57: 541-555.

972 Byrne S, Dundas CM, Kennedy MR, et al. (2009) Distribution of mid-latitude ground
973 ice on Mars from New impact craters. *Science* 325: 1674-1676.

974 Carr MH. (1987) Water on Mars. *Nature* 326: 30-35.

975 Carr MH. (2000) Martian oceans, valleys and climate. *Astron. Geophys.* 41: 3.20-23.26,
976 doi: 10.1046/j.1468-4004.2000.00320.x.

977 Carr MH and Schaber GG. (1977) Martian permafrost features. *J. Geophys. Res.* 82:
978 4039-4054.

979 Chapman MG. (2007) *The geology of Mars: evidence from Earth-based analogs*.
980 Cambridge: Cambridge University Press.

- Chicarro A, Martin P and Traunter R. (2004) Chicarro, A., Martin, P., Traunter, R. In: Wilson A (ed) *Mars Express: a European Mission to the Red Planet, SP-1240*. Noordwijk: European Space Agency Publication Division.
- Christensen P. (2003) Formation of recent martian gullies through melting of extensive water-rich snow deposits. *Nature* 422: 45-48.
- Conway SJ, Balme MR, Murray JB, et al. (2011a) The determination of martian gully formation processes by slope-area analysis. In: Balme MR, Bargery AS, Gallagher C, et al. (eds) *Martian Geomorphology*. London: Geological Society of London, Special Publications, 171-201.
- Conway SJ, Lamb MP, Balme MR, et al. (2011b) Enhanced runout and erosion by overland flow at low pressure and sub-freezing conditions: Experiments and application to Mars. *Icarus* 211: 443-457.
- Costard F, Forget F, Mangold N, et al. (2002) Formation of recent martian debris flows by melting of near-surface ground ice at high obliquity. *Science* 295: 110-113.
- Costard FM and Kargel JS. (1995) Outwash plains and thermokarst on Mars. *Icarus* 114: 93-112.
- Craddock RA and Howard AD. (2002) The case for rainfall on a warm, wet early Mars. *J. Geophys. Res.* 107: doi:10.1029/2001JE001505.
- Czudek T and Demek J. (1970) Thermokarst in Siberia and its influence on the development of lowland relief. *Quat. Res.* 1: 103-120.
- Dickson JL, Fassett CI and Head JW. (2009) Amazonian-aged fluvial valley systems in a climatic microenvironment on Mars: Melting of ice deposits on the interior of Lyot Crater. *Geophys. Res. Lett.* 36: doi:10.1029/2009GL037472.
- Dickson JL and Head JW. (2009) The formation and evolution of youthful gullies on Mars: Gullies as the late-stage phase of Mars' most recent ice age. *Icarus* 204: 63-86.
- Dickson JL, Head JW and Kreslavsky MA. (2007) Martian gullies in the southern mid-latitudes of Mars: Evidence for climate-controlled formation of young fluvial features based upon local and global topography. *Icarus* 188: 315-323.
- Diniega S, Byrne S, Bridges N, et al. (2010) Seasonality of present-day Martian dune-gully activity. *Geology* 38: 1047-1050.
- Doran PT, Lyons WB and McKnight DM. (2010) *Life in Antarctic Deserts and other Cold Dry Environments*. Cambridge: Cambridge University Press.
- Dundas CM, Keszthelyi LP, Bray VJ, et al. (2010a) Role of material properties in the cratering record of young platy-ridged lava on Mars. *Geophys. Res. Lett.* 37: doi:10.1029/2010GL042869.
- Dundas CM and McEwen AS. (2010) An assessment of evidence for pingos on Mars using HiRISE. *Icarus* 205: 244-258.
- Dundas CM, McEwen AS, Diniega S, et al. (2010b) New and recent gully activity on Mars as seen by HiRISE. *Geophys. Res. Lett.* 37: doi: 10.1029/2009GL041351.

1
2
3
4
5
6
7
8
9
10
11
12
13
14
15
16
17
18
19
20
21
22
23
24
25
26
27
28
29
30
31
32
33
34
35
36
37
38
39
40
41
42
43
44
45
46
47
48
49
50
51
52
53
54
55
56
57
58
59
60

1021 El Maarry MR, Markiewicz WJ, Mellon MT, et al. (2010) Crater floor polygons:
1022 Desiccation patterns of ancient lakes on Mars? *J. Geophys. Res.* 115: doi:
1023 10.1029/2010JE003609.
1024 Fairen AG. (2010) A cold and wet Mars. *Icarus* 208: 165-175.
1025 Fassett CI, Dickson JL, Head JW, et al. (2010) Supraglacial and proglacial valleys on
1026 Amazonian Mars. *Icarus*, 208, 86-100. *Icarus* 208: 86-100.
1027 Fastook JL, Head JW, Marchant DR, et al. (2012) Early Mars climate near the
1028 Noachian–Hesperian boundary: Independent evidence for cold conditions from
1029 basal melting of the south polar ice sheet (Dorsa Argentea formation) and
1030 implications for valley network formation. *Icarus* 219: 25-40.
1031 Feldman WC, Mellon MT, Gasnault O, et al. (2007) Vertical distribution of hydrogen at
1032 high northern latitudes on Mars: The Mars Odyssey Neutron Spectrometer.
1033 *Geophys. Res. Lett.* 34: doi:10.1029/2006GL028936.
1034 Feldman WC, Prettyman TH, Maurice S, et al. (2004) The global distribution of near-
1035 surface hydrogen on Mars. *J. Geophys. Res.* 109: doi:10.1029/2003JE002160.
1036 French HM. (2007) *The Periglacial Environment*, 3rd edn., Chichester: John Wiley and
1037 Sons.
1038 Gallagher C and Balme MR. (2011) Landforms indicative of ground-ice thaw in the
1039 northern high latitudes of Mars. In: Balme MR, Bargery AS, Gallagher CJ, et al.
1040 (eds) *Martian Geomorphology*. London: Geological Society of London Special
1041 Publications, 87-110.
1042 Gallagher C, Balme MR, Conway SJ, et al. (2011) Sorted clastic stripes, lobes and
1043 associated gullies in high-latitude craters on Mars: Landforms indicative of very
1044 recent, polycyclic ground-ice thaw and liquid flows. *Icarus* 211: 458-471.
1045 Golombek MP and Bridges NT. (2000) Erosion rates on Mars and implications for
1046 climate change: Constraints from the Pathfinder landing site. *J. Geophys. Res.*
1047 105: 1841-1853.
1048 Harris C. (1981) *Periglacial Mass-wasting: A review of Research*, Norwich:
1049 GeoAbstracts.
1050 Hartmann WK. (2007) Martian cratering 9: Toward resolution of the controversy about
1051 small craters *Icarus* 189: 274-278.
1052 Hartmann WK and Neukum G. (2001) Cratering Chronology and the Evolution of
1053 Mars. *Space Sci. Rev.* 96: 165-194.
1054 Hauber E, Reiss D, Ulrich M, et al. (2011a) Landscape evolution in Martian mid-
1055 latitude regions: insights from analogous periglacial landforms in Svalbard. In:
1056 Balme MR, Bargery AS, Gallagher CJ, et al. (eds) *Martian Geomorphology*.
1057 London: Geological Society of London, Special Publications, 111-131.
1058 Hauber E, Reiss D, Ulrich M, et al. (2011b) Periglacial landscapes on Svalbard:
1059 Terrestrial analogs for cold-climate landforms on Mars. In: Garry WB and

- 1060 Bleacher JE (eds) *Analogs for Planetary Exploration: Geological Society of*
 1061 *America Special Paper 483*. doi:10.1130/2011.2483(1112) in press.
- 1062 Hauber E, van Gasselt S, Chapman MG, et al. (2008) Geomorphic evidence for former
 1063 lobate debris aprons at low latitudes on Mars: Indicators of the Martian
 1064 paleoclimate. *J. Geophys. Res.* 113: doi:10.1029/2007JE002897.
- 1065 Head JW, Marchant DR, Dickson JL, et al. (2010) Northern mid-latitude glaciation in
 1066 the Amazonian period of Mars: Criteria for the recognition of debris-covered
 1067 glacier and valley glacier landsystem deposits. *Earth Planet. Sci. Lett.* 294: 306-
 1068 320.
- 1069 Head JW, Marchant DR and Kreslavsky MA. (2008) Formation of gullies on Mars:
 1070 Link to recent climate history and insolation microenvironments implicate
 1071 surface water flow origin *P. Natl. Acad. Sci. USA* 105: 13,258-213,263.
- 1072 Head JW, Mustard JF, Kreslavsky MA, et al. (2003) Recent ice ages on Mars. *Nature*
 1073 426: 797-802.
- 1074 Hecht MH. (2002) Metastability of water on Mars. *Icarus* 156: 373-386.
- 1075 Hecht MH, Kounaves SP, Quinn RC, et al. (2009) Detection of Perchlorate and the
 1076 Soluble Chemistry of Martian Soil at the Phoenix Lander Site. *Science* 325: 64-
 1077 67.
- 1078 Heldmann JL, Johansson H, Carlsson E, et al. (2005) Northern hemisphere gullies on
 1079 Mars: Analysis of spacecraft data and implications for formation mechanism.
 1080 XXXVI.
- 1081 Hess SL, Henry RM, Leovy CB, et al. (1977) Meteorological measurements from the
 1082 surface of Mars: Viking 1 and 2. *J. Geophys. Res.* 82: 4559-4574.
- 1083 Hill PR and Solomon S. (1999) Geomorphologic and Sedimentary Evolution of a
 1084 Transgressive Thermokarst Coast, Mackenzie Delta Region, Canadian Beaufort
 1085 Sea. *J. Coastal Res.* 15: 1011-1029.
- 1086 Holt JW, Safaeinili A, Plaut JJ, et al. (2008) Radar Sounding Evidence for Buried
 1087 Glaciers in the Southern Mid-Latitudes of Mars. *Science* 322: 1235-1238.
- 1088 Howard AD and Moore EJ. (2011) Late Hesperian to early Amazonian midlatitude
 1089 Martian valleys: Evidence from Newton and Gorgonum basins. *J. Geophys. Res.*
 1090 116: doi:10.1029/2010JE003782.
- 1091 Hubbard B, Milliken RE, Kargel JS, et al. (2011) Geomorphological characterisation
 1092 and interpretation of a mid-latitude glacier-like form: Hellas Planitia, Mars.
 1093 *Icarus* 211: 330-346.
- 1094 Hudson TL, Aharonson O, Schorghofer N, et al. (2007) Water vapor diffusion in Mars
 1095 subsurface environments. *J. Geophys. Res.* 112: doi:10.1029/2006JE002815.
- 1096 Ingersoll AP. (1970) Mars: Occurrence of liquid water. *Science* 168: 972-973.
- 1097 Irwin RP, Craddock RA and Howard AD. (2005) Interior channels in Martian valley
 1098 networks: Discharge and runoff production. *Geology* 33: 489-492.

1
2
3
4
5
6
7
8
9
10
11
12
13
14
15
16
17
18
19
20
21
22
23
24
25
26
27
28
29
30
31
32
33
34
35
36
37
38
39
40
41
42
43
44
45
46
47
48
49
50
51
52
53
54
55
56
57
58
59
60

1099 Jaeger WL, Keszthelyi LP, Skinner JA, et al. (2010) Emplacement of the youngest flood
1100 lava on Mars: A short, turbulent story. *Icarus* 205: 230–243.
1101 Jakosky BM. (2007) *An astrobiology strategy for the exploration of Mars*, Washington
1102 DC: National Academies Press.
1103 Jakosky BM and Farmer CB. (1982) The Seasonal and Global Behavior of Water Vapor
1104 in the Mars Atmosphere: Complete Global Results of the Viking Atmospheric
1105 Water Detector Experiment. *J. Geophys. Res.* 87: 2999-3019.
1106 Johnsson A, Reiss D, Hauber E, et al. (2011) Periglacial mass-wasting landforms on
1107 Mars suggestive of transient liquid water in the recent past: Insights from
1108 solifluction lobes on Svalbard. *Icarus*: in press.
1109 Johnsson A, Reiss D, Hauber E, et al. (2012) Periglacial mass-wasting landforms on
1110 Mars suggestive of transient liquid water in the recent past: Insights from
1111 solifluction lobes on Svalbard. *Icarus* 218: 489-505.
1112 Kessler MA and Werner BT. (2003) Self-Organization of Sorted Patterned Ground.
1113 *Science* 299: 380-383.
1114 Keszthelyi L, McEwen AS and Thordarson T. (2000) Terrestrial analogs and thermal
1115 models for Martian flood lavas. *J. Geophys. Res.* 105: 15027-15050.
1116 Keszthelyi L, Thordarson T, McEwen AS, et al. (2004) Icelandic analogs to Martian
1117 flood lavas. *Geochem. Geophys. Geosys.* 5: doi:10.1029/2004GC000758.
1118 Kieffer HH, Martin TZ, Peterfreund AR, et al. (1977) Thermal and albedo mapping of
1119 Mars during the Viking primary mission. *J. Geophys. Res.* 82: 4249-4291.
1120 Knauth LP and Burt D. (2002) Eutectic brines on Mars: origin and possible relation to
1121 young seepage features. *Icarus* 158: 267-271.
1122 Kneissl T, Reiss D, Van Gasselt S, et al. (2009) Distribution and orientation of
1123 northern-hemisphere gullies on Mars from the evaluation of HRSC and MOC-
1124 NA data. *Plan. Space Sci.* 294: 357-367.
1125 Kreslavsky MA. (2008) Slope steepness of channels and aprons: implications for origin
1126 of martian gullies. *Workshop on martian gullies: Theories and Tests*. LPI,
1127 Houston: #8034.
1128 Kreslavsky MA, Head JW and Marchant DR. (2008) Periods of active permafrost layer
1129 formation during the geological history of Mars: Implications for circum-polar
1130 and mid-latitude surface processes. *Plan. Space Sci.* 56: 289-302.
1131 Lanagan PD, McEwen AS, Keszthelyi L, et al. (2001) Rootless cones on Mars
1132 indicating the presence of shallow equatorial ground ice in recent times.
1133 *Geophysical Research Letters* 28: 2365-2367.
1134 Laskar J, Correia ACM, Gastineau M, et al. (2004) Long term evolution and chaotic
1135 diffusion of the insolation quantities of Mars. *Icarus* 170: 343-364.
1136 Lefort A, Russell PS, Thomas N, et al. (2009) Observations of periglacial landforms in
1137 Utopia Planitia with the High Resolution Imaging Science Experiment
1138 (HiRISE). *J. Geophys. Res.* 114: doi:10.1029/2008JE003264.

- 1139 Levy JS. (2012) Hydrological characteristics of recurrent slope lineae on Mars:
 1140 Evidence for liquid flow through regolith and comparisons with Antarctic
 1141 terrestrial analogs. *Icarus* 219: 1-4.
- 1142 Levy JS, Head JW and Marchant DR. (2009a) Thermal contraction crack polygons on
 1143 Mars: Classification, distribution, and climate implications from HiRISE
 1144 observations. *J. Geophys. Res.* 114: doi: 10.1029/2008JE003273.
- 1145 Levy JS, Head JW, Marchant DR, et al. (2009b) Geologically recent gully–polygon
 1146 relationships on Mars: Insights from the Antarctic Dry Valleys on the roles of
 1147 permafrost, microclimates, and water sources for surface flow. *Icarus* 209: 113-
 1148 126.
- 1149 Levy JS, Head JW, Marchant DR, et al. (2008) Identification of sublimation-type
 1150 thermal contraction crack polygons at the proposed NASA Phoenix landing site:
 1151 Implications for substrate properties and climate-driven morphological
 1152 evolution. *Geophys. Res. Lett.* 35: doi:10.1029/2007GL032813.
- 1153 Levy JS, Marchant DR and Head JW. (2010) Thermal contraction crack polygons on
 1154 Mars: A synthesis from HiRISE, Phoenix, and terrestrial analog studies. *Icarus*
 1155 206: 229-252.
- 1156 Li H, Robinson MS and Jurdy DM. (2005) Origin of martian northern hemisphere mid-
 1157 latitude lobate debris aprons. *Icarus* 176: 382-394.
- 1158 Lucchitta BK. (1981) Mars and Earth: Comparison of Cold Climate Features. *Icarus* 45:
 1159 264-303.
- 1160 Lucchitta BK. (1984) Ice and debris in the fretted terrain, Mars. *J. Geophys. Res.* 89(B1),
 1161 B409-B419. *J. Geophys. Res.* 89: B409-B419.
- 1162 Malin MC and Edgett KS. (2000) Evidence for recent groundwater seepage and surface
 1163 runoff on Mars. *Science* 288: 2330-2335.
- 1164 Malin MC, Edgett KS, Posiolova LV, et al. (2006) Present day impact cratering rate and
 1165 contemporary gully activity on Mars. *Science* 314: 1573-1577.
- 1166 Mangold N. (2005) High latitude patterned ground on Mars: Classification, distribution
 1167 and climatic control. *Icarus* 174: 336-359.
- 1168 Mangold N, Mangeney A, Migeon V, et al. (2010) Sinuous gullies on Mars: Frequency,
 1169 distribution, and implications for flow properties. *J. Geophys. Res.* 115: doi:
 1170 10.1029/2009JE003540.
- 1171 Mangold N, Quantin C, Ansan V, et al. (2004) Evidence for Precipitation on Mars from
 1172 Dendritic Valleys in the Valles Marineris Area *Science* 305: 78-81.
- 1173 Marchant DR and Head JW. (2007) Antarctic dry valleys: Microclimate zonation,
 1174 variable geomorphic processes, and implication for assessing climate change on
 1175 Mars. *Icarus* 192: 187-222.
- 1176 Marion GM, Catling DC, Claire M, et al. (2009) Modeling aqueous perchlorate
 1177 chemistries with application to Mars. *Lunar Plan. Sci. XL [CDROM]*: Abstr.
 1178 1959.

1
2
3
4
5
6
7
8
9
10
11
12
13
14
15
16
17
18
19
20
21
22
23
24
25
26
27
28
29
30
31
32
33
34
35
36
37
38
39
40
41
42
43
44
45
46
47
48
49
50
51
52
53
54
55
56
57
58
59
60

1179 Marquez A, Fernandez C, Anguita F, et al. (2004) New evidence for a volcanically,
1180 tectonically, and climatically active Mars. *Icarus* 172: 573-581.
1181 Matsuoka N. (2011) Climate and material controls on periglacial soil processes: Toward
1182 improving periglacial climate indicators. *Quat. Res.* 75: 356-365.
1183 McEwen AS and Bierhaus EB. (2006) The importance of secondary cratering to age
1184 constraints on planetary surfaces. *Annu. Rev. Earth Planet. Sci.* 34: 535-567.
1185 McEwen AS, Ojha L, Dundas CM, et al. (2011) Seasonal flows on warm Martian
1186 slopes. *Science* 333: 740-743.
1187 Mellon MT. (1997) Small-scale polygonal features on Mars: Seasonal thermal
1188 contraction cracks in permafrost. *J. Geophys. Res.* 102: 25,617-625,628.
1189 Mellon MT, Arvidson RE, Marlow JJ, et al. (2008) Periglacial landforms at the Phoenix
1190 landing site and the northern plains of Mars. *J. Geophys. Res.* 113:
1191 doi:10.1029/2007JE003039.
1192 Milliken RE, Mustard JF and Goldsby DL. (2003) Viscous flow features on the surface
1193 of Mars: Observation from high-resolution Mars Orbiter Camera (MOC) images.
1194 *J. Geophys. Res.* 108: doi:10.1029/2002JE002005.
1195 Möhlmann DTF. (2010) Temporary liquid water in upper snow/ice sub-surfaces on
1196 Mars? . *Icarus* 207: 140-148.
1197 Möhlmann DTF and Thomsen K. (2011) Properties of cryobrines on Mars. *Icarus* 212:
1198 123-130.
1199 Morgenstern A, Hauber E, Reiss D, et al. (2007) Deposition and degradation of a
1200 volatile-rich layer in Utopia Planitia, and implications for climate history on
1201 Mars. *J. Geophys. Res.* 112: doi:10.1029/2006JE002869.
1202 Murchie S and the CRISM Science Team. (2007) Compact Reconnaissance Imaging
1203 Spectrometer for Mars (CRISM) on Mars Reconnaissance Orbiter (MRO). *J.*
1204 *Geophys. Res.* 112: doi:10.1029/2006JE002682.
1205 Murton JB and Kolstrup E. (2003) Ice-wedge casts as indicators of paleotemperatures:
1206 precise proxy or wishful thinking? *Prog. Phys. Geog.* 27: 155-170.
1207 Musselwhite DS, Swindle TD and Lunine J. (2001) Liquid CO₂ breakout and the
1208 formation of recent small channels on Mars. *Geophysical Research Letters* 28:
1209 1283-1285.
1210 Orloff TC, Kreslavsky M, Asphaug E, et al. (2011) Boulder movement at high northern
1211 latitudes of Mars. *J. Geophys. Res.* 115: doi:10.1029/2011JE003811
1212 Orloff TC, Kreslavsky MA and Asphaug EI. (2012) Possible mechanism for boulder
1213 clustering on thermal contraction polygons. *Lunar Plan. Sci. Conf. XLIII,*
1214 *Houston, Texas:* Abstr. 1652.
1215 Owen T, Biemann K, Rushnek DR, et al. (1977) The composition of the atmosphere at
1216 the surface of Mars. *J. Geophys. Res.* 82.
1217 Page DP. (2007) Recent low-latitude freeze-thaw on Mars. *Icarus* 189: 83-117.

- 1218 Page DP and Murray JB. (2006) Stratigraphical and morphological evidence for pingo
1219 genesis in the Cerberus plains. *Icarus* 183: 46-54.
- 1220 Pelletier JD, Kolb KJ, McEwen AS, et al. (2008) Recent bright gully deposits on Mars:
1221 Wet or dry flow? *Geology* 36: 211-214.
- 1222 Pestova O, Myund L, Khripun M, et al. (2005) Polythermal Study of the Systems
1223 $M(\text{ClO}_4)_2 \cdot \text{H}_2\text{O}$ ($M^{2+} = \text{Mg}^{2+}, \text{Ca}^{2+}, \text{Sr}^{2+}, \text{Ba}^{2+}$). *Russ. J. Appl. Chem.* 78: 409-
1224 413.
- 1225 Plaut JJ, Safaeinili A, Holt JW, et al. (2009) Radar evidence for ice in lobate debris
1226 aprons in the mid-northern latitudes of Mars. *Geophys. Res. Lett.* 36:
1227 doi:10.1029/2008GL036379.
- 1228 Plescia JB. (1990) Recent flood lavas in the Elysium region of Mars. *Icarus* 88: 465-
1229 490.
- 1230 Read PL and Lewis SR. (2004) *The Martian Climate Revisited: Atmosphere and*
1231 *Environment of a Desert Planet*, Berlin: Springer.
- 1232 Reiss D, Erkeling G, Bauch KE, et al. (2010) Evidence for present day gully activity on
1233 the Russell crater dune field, Mars. *Geophys. Res. Lett.* 37: doi:
1234 10.1029/2009GL042192.
- 1235 Reiss D, Hauber E, Hiesinger H, et al. (2011) Terrestrial gullies and debris-flow tracks
1236 on Svalbard as planetary analogs for Mars. In: Barry WB and Bleacher JE (eds)
1237 *Analogs for Planetary Exploration: Geological Society of America Special*
1238 *Paper 483*. Geological Society of America, 567.
- 1239 Reiss D, Hiesinger H, Hauber E, et al. (2009) Regional differences in gully occurrence
1240 on Mars: A comparison between the Hale and Bond craters. *Plan. Space Sci.* 57:
1241 958-974.
- 1242 Reiss D, van Gasselt S, Neukum G, et al. (2004) Absolute dune ages and implications
1243 for the time of formation of gullies in Nirgal Vallis, Mars. *J. Geophys. Res.* 109:
1244 doi:10.1029/2004JE002251.
- 1245 Rossbacher LA and Judson S. (1981) Ground ice on Mars: Inventory, distribution, and
1246 resulting landforms. *Icarus* 45: 39-59.
- 1247 Russell PS and Head JW. (2007) The Martian hydrologic system: Multiple recharge
1248 centers at large volcanic provinces and the contribution of snowmelt to outflow
1249 channel activity. *Plan. Space Sci.* 55: 315-332.
- 1250 Ryan JR and Christensen P. (2012) Coils and Polygonal Crust in the Athabasca Valles
1251 Region, Mars, as Evidence for a Volcanic History. *Science* 336: 449-452.
- 1252 Schorghofer N and Aharonson O. (2005) Stability and exchange of subsurface ice on
1253 Mars. *J. Geophys. Res.* 110: doi:10.1029/2004JE002350.
- 1254 Seibert NM and Kargel JS. (2001) Small-scale martian polygonal terrain: Implications
1255 for liquid surface water. *Geophys. Res. Lett* 28: 899-902.

1
2
3
4
5
6
7
8
9
10
11
12
13
14
15
16
17
18
19
20
21
22
23
24
25
26
27
28
29
30
31
32
33
34
35
36
37
38
39
40
41
42
43
44
45
46
47
48
49
50
51
52
53
54
55
56
57
58
59
60

1256 Séjourné A, Costard F, Gargani J, et al. (2011) Scalloped depressions and small-sized
1257 polygons in western Utopia Planitia, Mars: A new formation hypothesis. *Plan.*
1258 *Space Sci.* 59: 412-422.

1259 Shean DE. (2010) Candidate ice-rich material within equatorial craters on Mars.
1260 *Geophys. Res. Lett.* 37: doi:10.1029/2010GL045181

1261 Snyder CW and Moroz VI. (1992) Spacecraft exploration of Mars. In: Kieffer HH,
1262 Jakosky BM, Snyder CW, et al. (eds) *Mars*. Tucson: University of Arizona
1263 Press.

1264 Soare RJ, Burr DM and Wan Bun Tseung J-M. (2005) Possible pingos and a periglacial
1265 landscape in northwest Utopia Planitia. *Icarus* 174: 373-382.

1266 Soare RJ, Kargel JS, Osinski GR, et al. (2007) Thermokarst processes and the origin of
1267 crater-rim gullies in Utopia and western Elysium Planitia. *Icarus* 191: 95-112.

1268 Soare RJ, Osinski GR and Roehm CL. (2008) Thermokarst lakes and ponds on Mars in
1269 the very recent (late Amazonian) past. *Earth Planet. Sci. Lett* 272: 382-393.

1270 Souness C, Hubbard B, Milliken RE, et al. (2012) An inventory and population-scale
1271 analysis of martian glacier-like forms. *Icarus* 217: 243-255.

1272 Squyres SW. (1979) The distribution of lobate debris aprons and similar flows on Mars.
1273 *J. Geophys. Res.* 84: 8087-8096.

1274 Squyres SW and Carr MH. (1986) Geomorphic evidence for the distribution of ground
1275 ice on Mars. *Science* 231: 249-252.

1276 Tanaka KL, Chapman MG and Scott DH. (1992) Geologic map of the Elysium region
1277 of Mars. *U.S. Geol. Surv. Misc. Invest. Ser.:* MAP I-2147.

1278 Treiman AH. (2003) Geologic settings of Martian gullies: implications for their origins.
1279 *J. Geophys. Res.* 108: doi:10.1029/1202JE001900.

1280 Twidale CR. (1999) Landforms ancient and recent: the paradox. *Geogr. Ann. A* 81A:
1281 431-441.

1282 Ulrich M, Hauber E, Herzs Schuh U, et al. (2011) Polygon pattern geomorphometry on
1283 Svalbard (Norway) and western Utopia Planitia (Mars) using high-resolution
1284 stereo remote-sensing data. *Geomorphology* 134: 197-216.

1285 Ulrich M, Morgenstern A, Günther F, et al. (2010) Thermokarst in Siberian ice-rich
1286 permafrost: Comparison to asymmetric scalloped depressions on Mars. *J.*
1287 *Geophys. Res.* 115: doi:10.1029/2010JE003640.

1288 Vincendon M, Mustard J, Forget F, et al. (2010) Near-tropical subsurface ice on Mars.
1289 *Geophys. Res. Lett.* 37: doi:10.1029/2009GL041426.

1290 Williams KE, Toon OB, Heldmann JL, et al. (2009) Ancient melting of mid-latitude
1291 snowpacks on Mars as a water source for gullies. *Icarus* 200: 418-425.

1292 Zanetti M, Hiesinger H, Reiss D, et al. (2010) Distribution and evolution of scalloped
1293 terrain in the southern hemisphere. *Icarus* 206: 691-706.

- 1
2
3
4
5
6
7
8
9 1294 Zent AP, Hecht MH, Cobos DR, et al. (2010) Initial results from the thermal and
10 1295 electrical conductivity probe (TECP) on Phoenix. *J. Geophys. Res.* 115:
11 1296 doi:10.1029/2009JE003420, 002010.
12 1297 Zurek RW and Smrekar SE. (2007) An overview of the Mars Reconnaissance Orbiter
13 1298 (MRO) science mission. *J. Geophys. Res.* 112: doi:10.1029/2006JE002701.
14 1299
15 1300
16
17
18
19
20
21
22
23
24
25
26
27
28
29
30
31
32
33
34
35
36
37
38
39
40
41
42
43
44
45
46
47
48
49
50
51
52
53
54
55
56
57
58
59
60

1
2
3
4
5
6
7
8
9
10
11
12
13
14
15
16
17
18
19
20
21
22
23
24
25
26
27
28
29
30
31
32
33
34
35
36
37
38
39
40
41
42
43
44
45
46
47
48
49
50
51
52
53
54
55
56
57
58
59
60

1 Figure/table captions for “Morphological evidence for geologically recent thaw of ice on
2 Mars: case studies from very high resolution imaging data”

3
4 Figure 1. Dendritic valley networks in the cratered martian highlands, indicating a wetter
5 climate in the ancient past. The formation of such fluvial valleys sharply declined between 3.8
6 Ga and 3.5 Ga at the end of the ‘Noachian’ epoch (HRSC false colour image of orbit
7 h0532_0000; the large crater has a diameter of ~45 km and is centred at 12.43°S and
8 60.57°E). North is up in this and all other images unless otherwise stated or demonstrated by a
9 north-arrow. Image credit ESA/DLR/FUB.

10
11 Figure 2. The martian obliquity cycle over the last 20 Ma. Obliquity changes by nearly 20° on
12 an ~ 100 ka cycle (see inset). The magnitude of these obliquity changes vary on ~1 and ~2 Ma
13 cycles. The mean obliquity changed from about 35° to about 25° at about 5 Ma, as shown by
14 the dotted line (after Laskar et al., 2004). Prior to 20 Ma the obliquity is not well-constrained
15 by models.

16
17 Figure 3. Examples of landforms on Mars that might have formed by thaw. a) martian
18 hillslope gully at 38.58S, 319.88E (HiRISE image PSP_006888_1410). Note the alcove at the
19 top of the slope, and the sinuous channels and debris fan at the foot of the slope. Illumination
20 is from the left and north is up in this and all following Mars images unless otherwise
21 specified. b) Gully and debris flow features on Earth (Hannaskogdalen, Svalbard) that are
22 morphologically similar to the martian gullies. Svalbard image is an aerial photograph from
23 the German DLR airborne ‘HRSC-AX’ camera (Hauber et al., 2011b). c-e) Time-series
24 showing recurring slope lineae on the inner crater wall of Newton Crater near 41.6°S,
25 202.3°E. The lineae are the dark, finger-like structures that can be seen in d and e. Figure 3c
26 shows the location before the lineae began. Dark arrows in d and e show the end points of the
27 lineae, pale arrows indicate the position of these termini from the image before. The time
28 series covers about 100 martian days (“sols”) in total, and images d and e are separated by 35
29 sols. The lineae have therefore progressed at a rate of 1 m per day (HiRISE images
30 PSP_0021555_1380; PSP_0022267_1380; PSP_0022689_1380). f) Lobate features on the
31 inner wall of an impact crater on Mars near 71.98N, 344.58E (HiRISE PSP_010077_2520). g)
32 Solifluction lobes on the slopes of Louisfjellet (Svalbard). Note the striking similarity in scale

and morphology between d) and e). Images a, b, d, and e are after Figures 3 and 6 in Hauber (2011a). Image credits: NASA/JPL/UofA and DLR.

Figure 4. Evidence for seasonal precipitation at martian mid-latitudes. A crater at 46.05°S and 183.85°E is shown at different seasons (seasons on Mars are indicated by solar longitude, L_S , with $L_S=0$ corresponding to the beginning of northern spring and a whole year being equivalent to 360°). Only pole-facing slopes in scenes acquired in southern winter (show bright deposits interpreted as water ice (cf. Vincendon et al., 2010). These locations correspond to places where periglacial-like features are preferentially observed. (a-c) HRSC false-colour views (image numbers: a-h2630_0001, b-h6547_0000, c-h8569_0000). (d-f) CTX images (image numbers: a-B11_013934_1337, b-P04_002779_1337, c-G03_019314_1337). Image credits NASA/JPL/UofA/MSSS

Figure 5. Examples of typical ice-related landforms in martian mid-latitudes. (a) Viscous flow features in Deuteronilus Mensae at the dichotomy boundary. The features indicate plastic deformation and resemble terrestrial glaciers. The perspective view towards North was generated from HRSC stereo scene h8289_0000 and is located at ~40°N and 23°E. (b) Small valleys downslope of viscous flow features (upper right; interpreted as rock glaciers). Arrows indicate inferred flow direction. Such valleys have been interpreted as glaciofluvial valleys formed by meltwater by Fassett et al. (2010) (detail of CTX image P04_002676_1413; centred at 38.24°S and 113.12°E). (c) Landforms typical of Utopia Planitia, Mars. Asymmetric scalloped depressions display steeper pole-facing slopes and cut large polygons that dissect the surrounding plains. Smaller polygons (see inset) overprint the depressions, indicating that landform evolution went on even after the degradation of the ice-rich substrate. Detail of HiRISE image PSP_001872_2260, centred near 45.6°N and 93.7°E. (d) Fractured mound that morphologically resembles pingos on Earth. The mound is located on a crater floor near 31.8°S and 347.2°E (detail of HiRISE image PSP_007533_1480). (e) Two scales of polygons on a crater floor near 64.5°N and 67.3°E (detail of HiRISE image PSP_008492_2450). Image credits NASA/JPL/UofA/MSSS and ESA/DLR/FUB

Figure 6. Assemblage of cold-climate features in a mid-latitude crater (detail of HiRISE image PSP_001684_1410; near 38.9°S and 196°E). a) Gullies (ravines) and associated fan deposits. b) Stripes oriented downslope. It is not possible to determine if the stripes are sorted

1
2
3
4
5
6
7
8
9
10
11
12
13
14
15
16
17
18
19
20
21
22
23
24
25
26
27
28
29
30
31
32
33
34
35
36
37
38
39
40
41
42
43
44
45
46
47
48
49
50
51
52
53
54
55
56
57
58
59
60

66 or not. c) Lobe-like features (arrows) indicative of downslope creep. Image credits
67 NASA/JPL/UofA.

68
69 Figure 7. Sorted forms within and around Heimdal crater showing trends in morphology and
70 clast abundance. The clastic areas appear cut by later fractures in all cases. Approximate slope
71 measurements are given in bottom left corner of each panel. All images are lit from the lower
72 left. (a) Clastic stripes on a steep slope on the inner crater wall of Heimdal crater. HiRISE
73 image PSP_009580_2485. (b) Clastic polygons trending into clastic stripes on the outer crater
74 wall. HiRISE image PSP_009079_2485. (c) Clastic rubble piles or ‘islands’ near the base of
75 the inner crater wall. HiRISE image PSP_009778_2485. (d) Low-albedo polygons inferred to
76 comprise sorted clasts below the image resolution. These polygons appear to be somewhat
77 high-centred. HiRISE image PSP_009079_2485. Image credits NASA/JPL/UofA. After
78 Figure 3 in Gallagher et al. (2011).

79
80 Figure 8. Landform assemblage on the inner walls of Heimdal crater. a). The upper part of the
81 image shows the crater rim, and the lower part the crater interior. Lobate, clastic forms (b and
82 blockfields (c) can be seen. Blockfields near the crater rim trend into linear and lobate forms
83 (downslope of the blockfield in c), and linear slope-parallel forms (throughout the centre of
84 the image; see also Figure 7a), are all visible and in b) trend into lobate forms. Nearer the base
85 of the inner crater wall the slope is less and the surface appears rougher, perhaps pitted in
86 places, and contains fewer organised clastic landforms. Part of HiRISE image
87 PSP_009778_2438. Image credits NASA/JPL/UofA.

88
89 Figure 9. a) Stone banked lobes incised by gullies on the interior slopes of a crater at $\sim 59.5^\circ$
90 N 302.4° E; boxes show relative locations of Figs. 9b, d and e. Lobes are characterised by
91 bright treads and dark, clastic risers. In places, lobe assemblages give way to polygonally
92 fractured ground of more uniform tone (P), although subtle albedo variation suggests that this
93 ground may be the reworked continuation of the adjacent lobes. Gully-fan systems (Q) have
94 incised many of the lobes, wiping-out some completely while only partially deflating others.
95 b) Lobes exhibiting bright, fine textured low angle treads bounded by dark, steeper clastic
96 risers; box shows relative location of Fig. 9c. c) Clastic lobes are fed by slope-parallel clastic
97 stripes. Interlobate surfaces show a more pronounced fracture pattern (visible also in Fig. 9b
98 more broadly), suggesting that the lobes here are accumulations overlying fractured ground.
99 d) Lobe deflation by a gully rill with a small distal, fan-like, sediment accumulation (X). The

next clastic riser downslope (Y) has been deflated by branching gully rills, demonstrating that solifluction was succeeded by liquid flow across the surface. e) Axial gully and rills have incised a texturally fine tread (A) but only partly deflated the clastic riser (B). The sudden introduction of these eroded and winnowed sediments probably caused the transport capacity of the gully system to be exceeded where the gradient of the gully diminished on the next tread downslope, triggering deposition of the fan on this surface (C). Parts of HiRISE image PSP_007666_2400. Image credit NASA/JPL/UofA. After Fig 14 in Gallagher et al. (2011) Figure 14.

Figure 10. Planview images showing the Athabasca Vallis source area. a) Context view showing segments of the Cerberus Fossae fracture system (A), the apparent twin source regions (C, D) of Athabasca Vallis, and the extent of Figure 10b (marked by the white box). The darker toned surfaces match the mapped extents of the channel floor. The white arrow indicates the direction of flow; Athabasca Vallis extends for ~ 250 km in this direction. Part of HRSC nadir image h1196. b) Higher resolution view of a part of the western source region. White boxes labelled P, Q, R show the locations of Figures 12, 11, and 13 respectively. Mosaic of HiRISE images PSP_007843_1905 and PSP_009280_1905. Image credit NASA/JPL/UofA and ESA/DLR/FUB. After Balme and Gallagher (2009).

Figure 11. Scarps at the margin of a low-relief, polygonally patterned surface (P). The scarps contain multiple small amphitheatre-shaped niches containing smooth material (Q), and are fronted by accumulations of meter scale clasts (R), and contributory channel networks (S). Note the “spurs” protruding from the sides of the niches. The channels appear incised into a faintly polygonised surface and terminate in a hummocky deposit in a low basin (T). There is a possibly leveed flow-like feature (arrowed) within the channel terminal deposits. Part of HiRISE image PSP_009280_1905. Image credit NASA/JPL/UofA. After Balme and Gallagher (2009).

Figure 12. Niche-indented scarps surrounding linked basins. Here, the topographically highest polygonised surfaces (A) appear to have degraded to form shallow basins. The shallowest depressions have polygonised floors, as do the outer floors of deeper depressions (B). Several of the larger basins have roughly textured floors, sometimes containing mound/cone landforms (C). The small image, lower right, shows a higher resolution view of one of these basins (in the white box) and reveals cone-like landforms (X) and incised gullies

1
2
3
4
5
6
7
8
9
10
11
12
13
14
15
16
17
18
19
20
21
22
23
24
25
26
27
28
29
30
31
32
33
34
35
36
37
38
39
40
41
42
43
44
45
46
47
48
49
50
51
52
53
54
55
56
57
58
59
60

134 on the slopes of the basin beneath the headscarp. Small gullies are also seen at Y. A single
135 outflow channel from a shallow, polygonised depression is shown at Z, and could be a
136 “tapping” channel via which fluid drained the depression. The topographically lowest part of
137 the scene (D) has a more subdued texture than the other polygonised surfaces. Part of HiRISE
138 image PSP_007843_1905. Image credit NASA/JPL/UofA. After Balme and Gallagher (2009).
139
140 Figure 13. Shallow, composite basin within the main Athabasca Vallis channel. The basin
141 appears to have formed by the merging of other small basins that grew in the polygonally
142 patterned ground (A), as shown by the causeways and remnant headlands (B) of polygonised
143 material. It is clear that development of individual basins was accompanied within by the
144 formation of moated, conical landforms, strengthening the interpretation of these forms as
145 pingos. At the west, scarp-parallel ridges beneath the headscarp (X) appear similar to
146 terrestrial subsidence failures. A prominent channel enters the basin to the north at Y. The
147 floor of the basin is dominated by cone/mound landforms. Part of HiRISE image
148 PSP_009280_1905. Image credit NASA/JPL/UofA. After Balme and Gallagher (2009).
149
150 Table 1. Possible periglacial landforms on Mars.
151

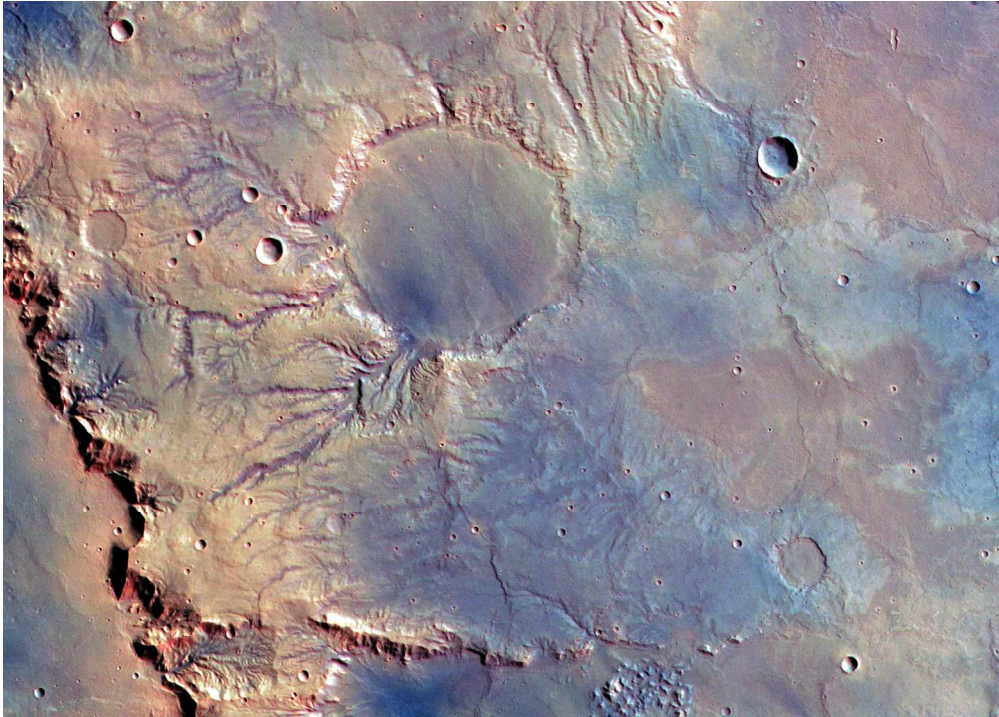


Figure 1
150x107mm (300 x 300 DPI)

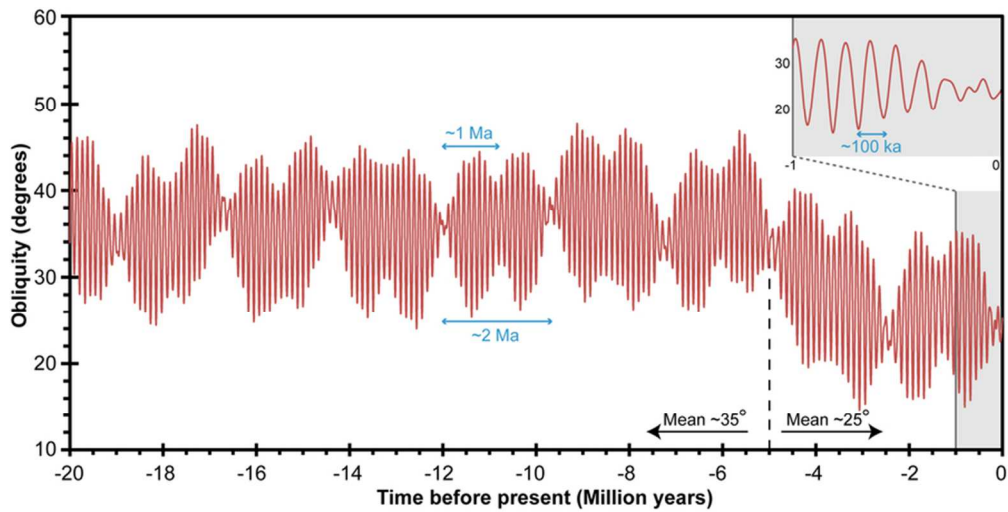
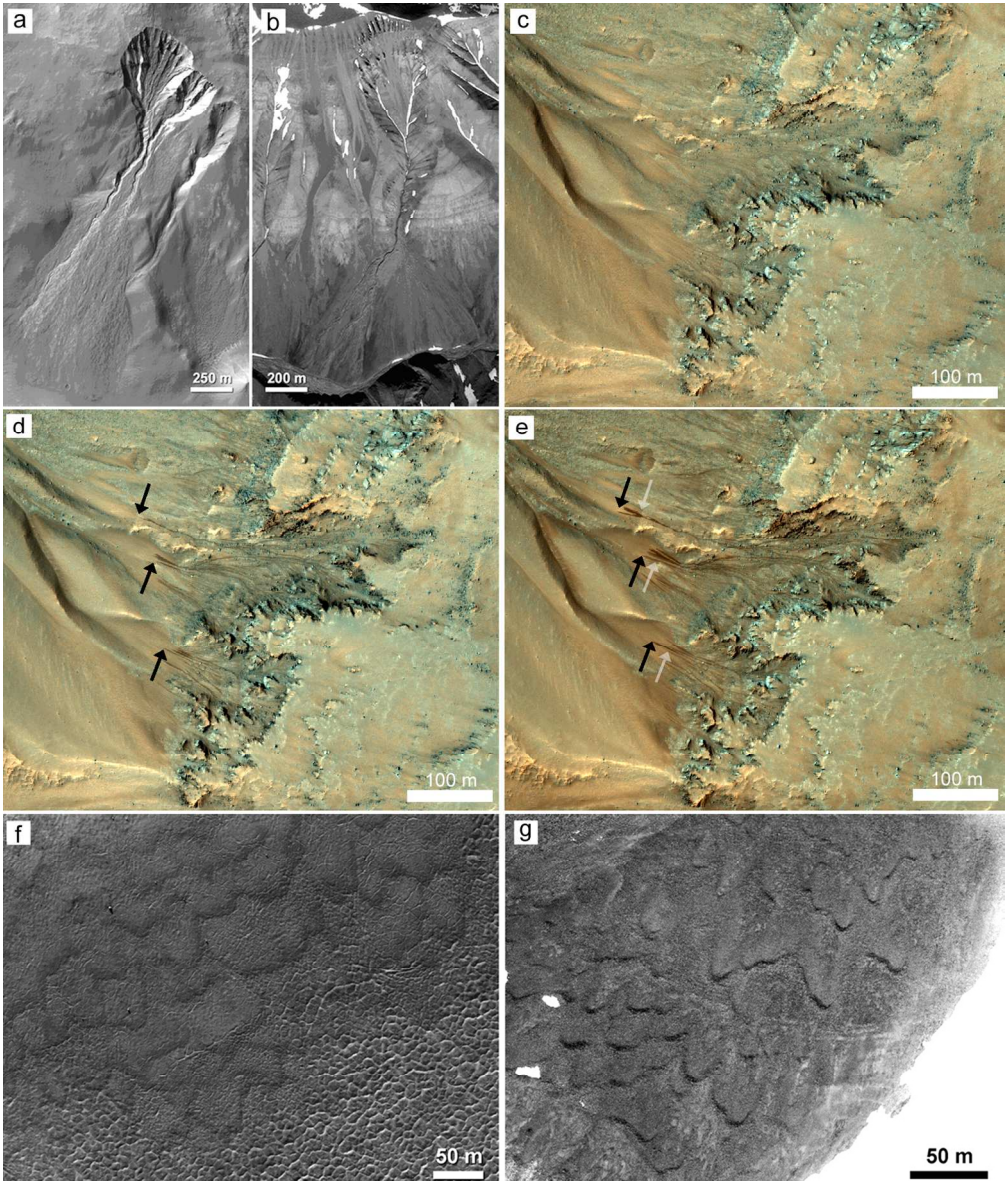


Figure 2
75x38mm (300 x 300 DPI)



149x175mm (300 x 300 DPI)

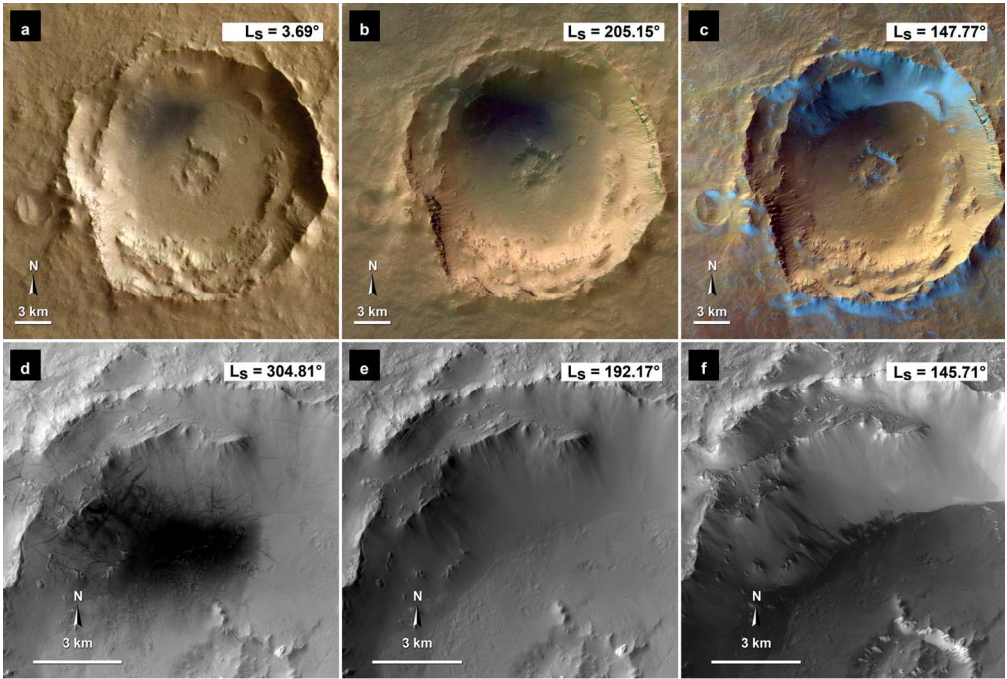


Figure 4
150x101mm (300 x 300 DPI)

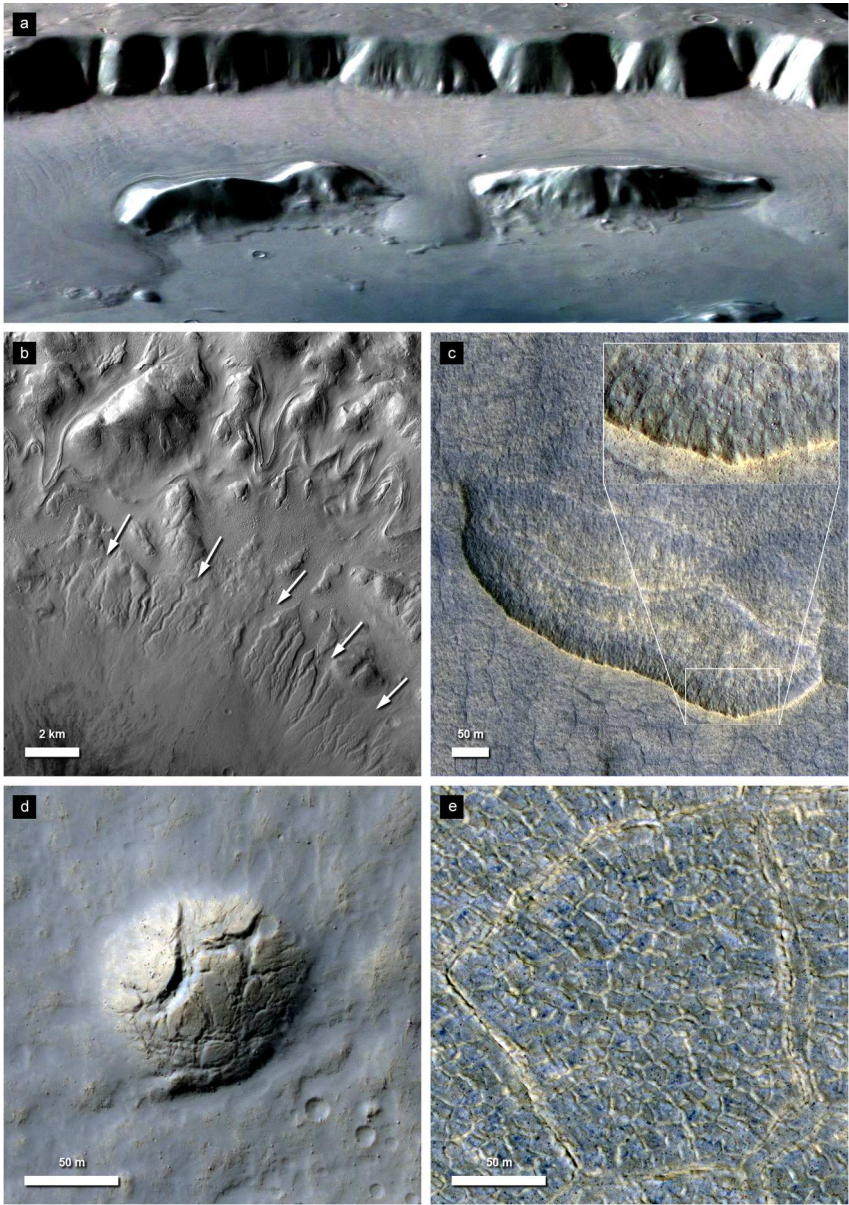


Figure 5
150x213mm (300 x 300 DPI)

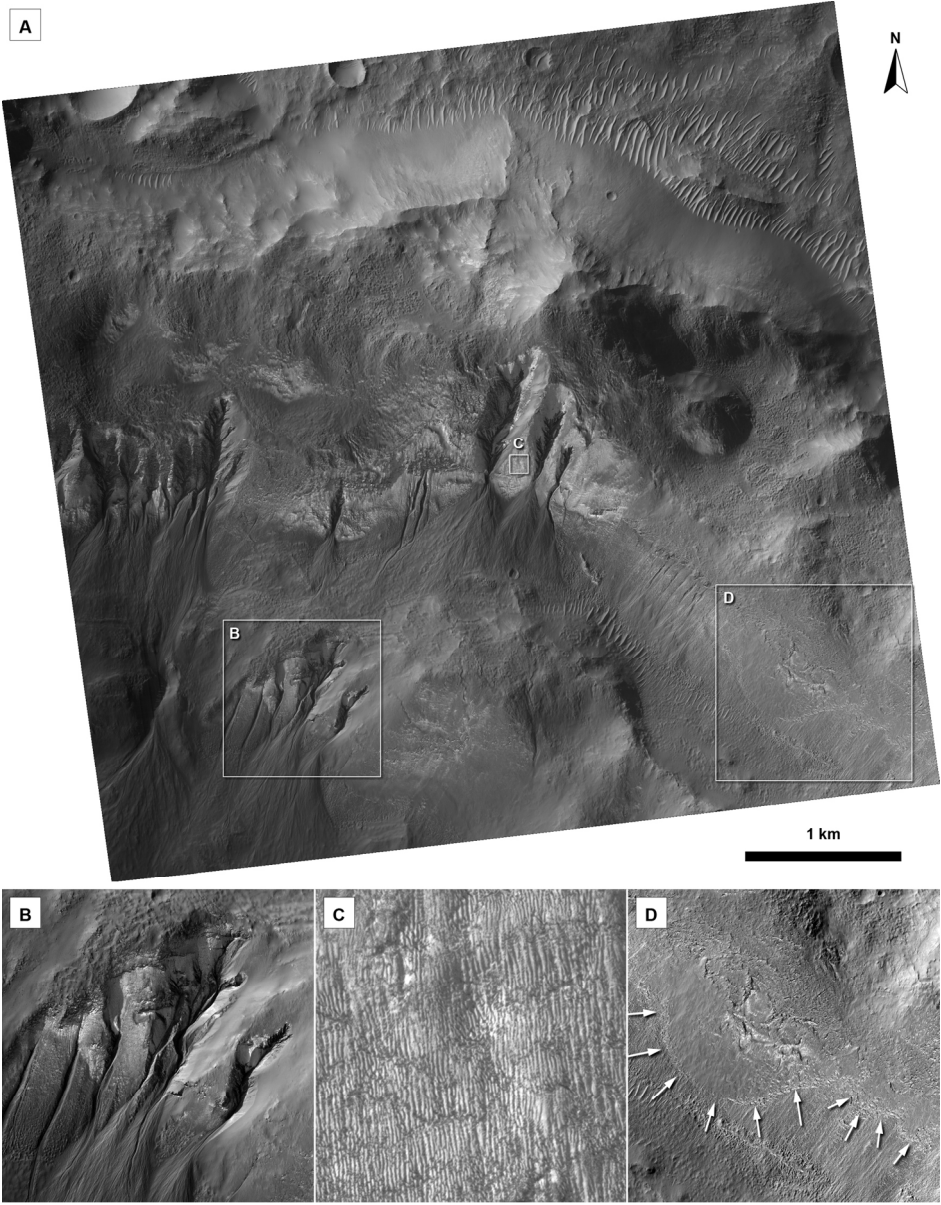


Figure 6
150x191mm (300 x 300 DPI)

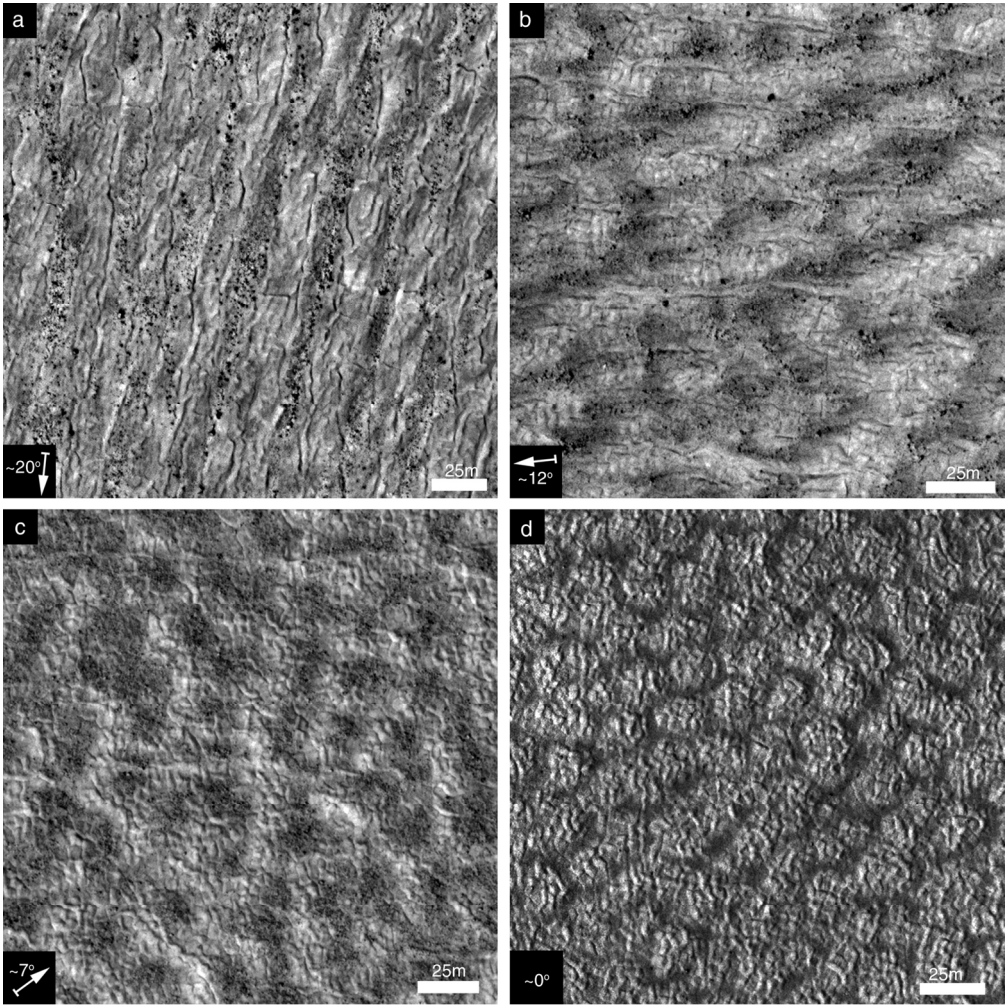


Figure 7
150x150mm (300 x 300 DPI)



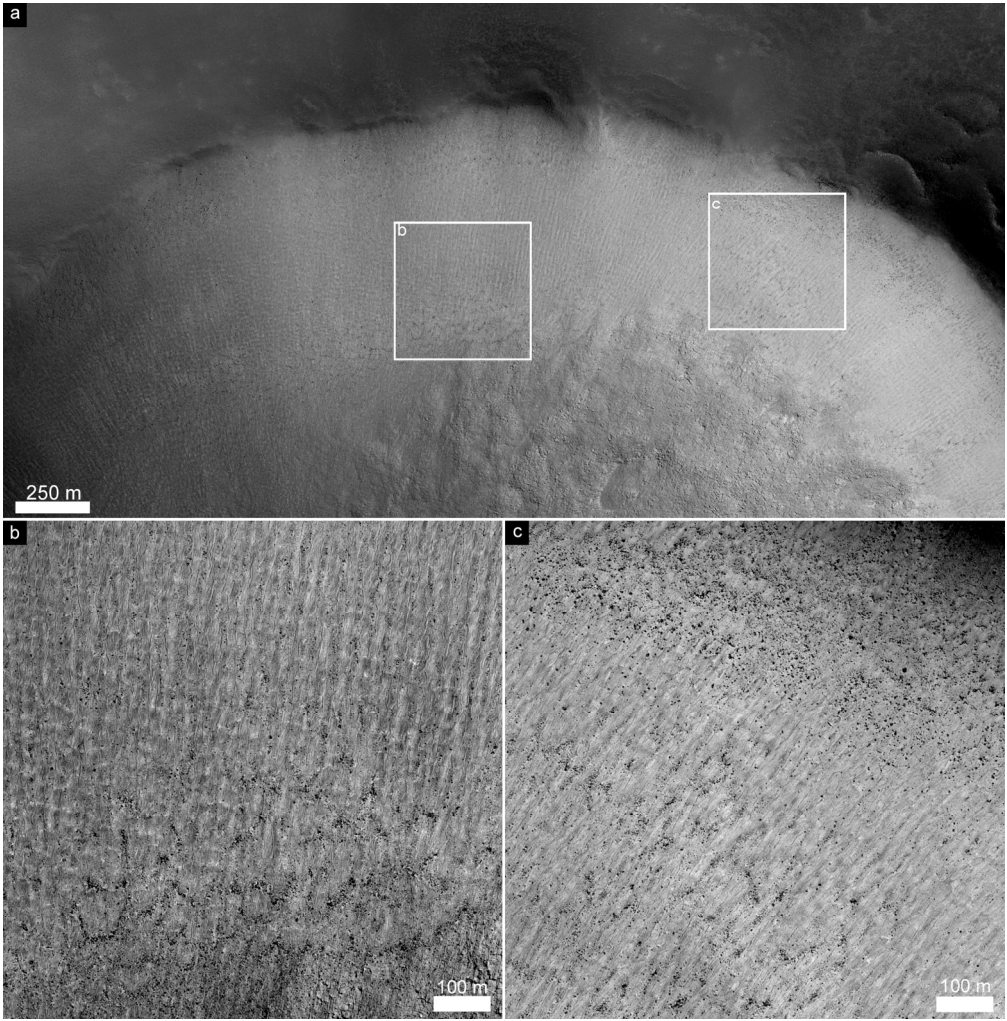


Figure 8
152x155mm (300 x 300 DPI)



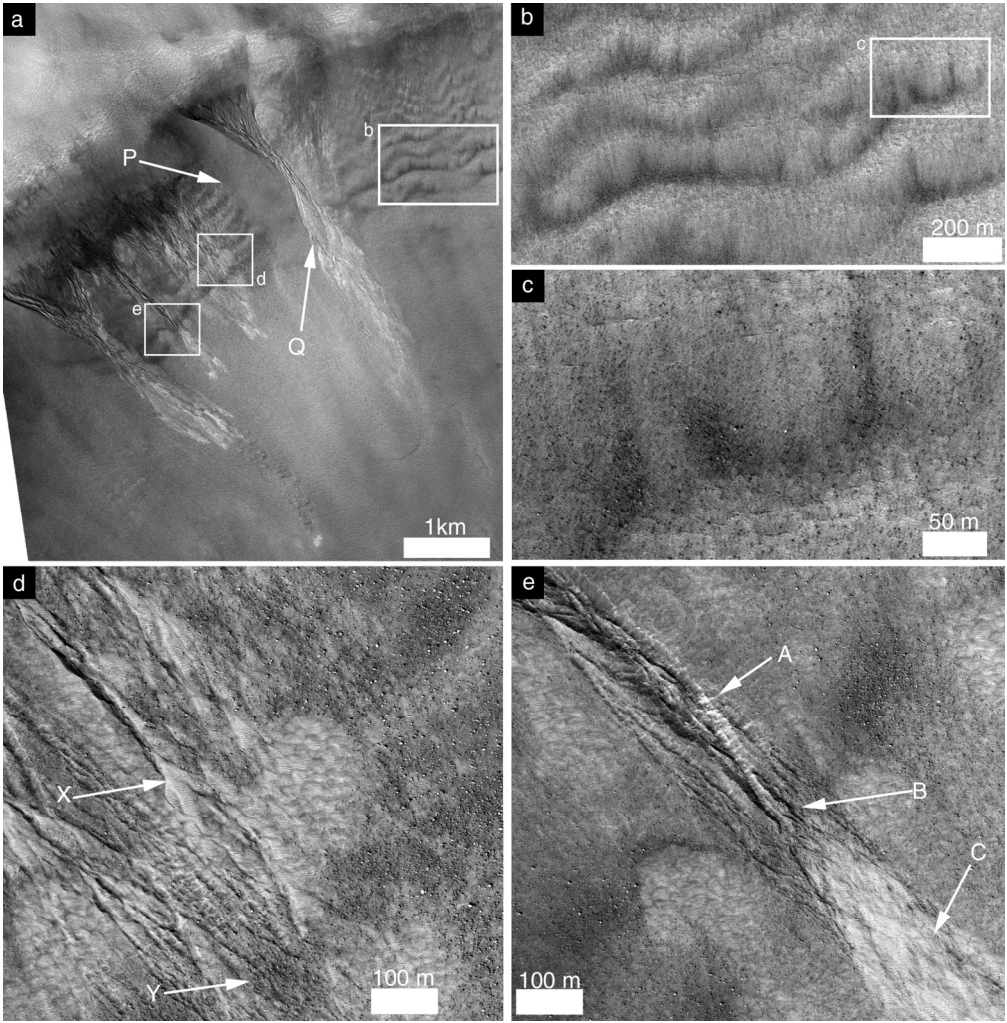


Figure 9
158x161mm (300 x 300 DPI)

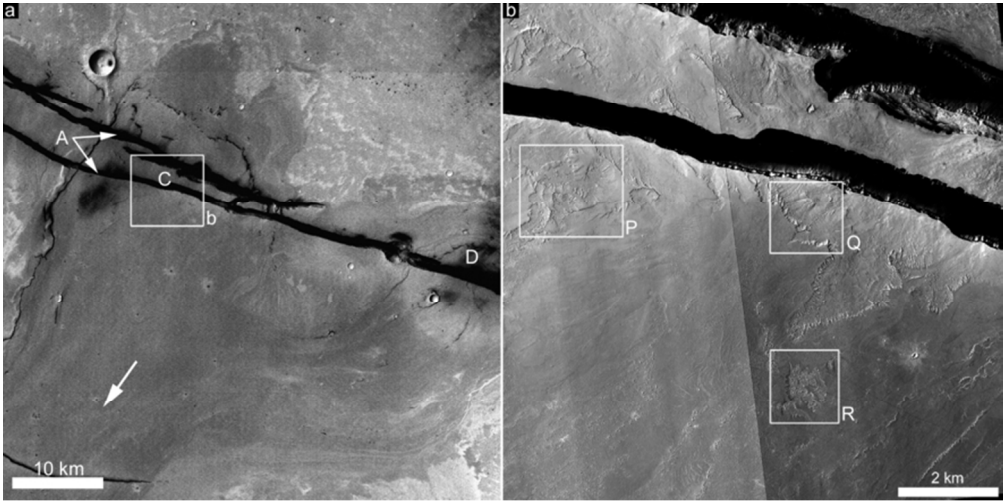


Figure 10
74x37mm (300 x 300 DPI)

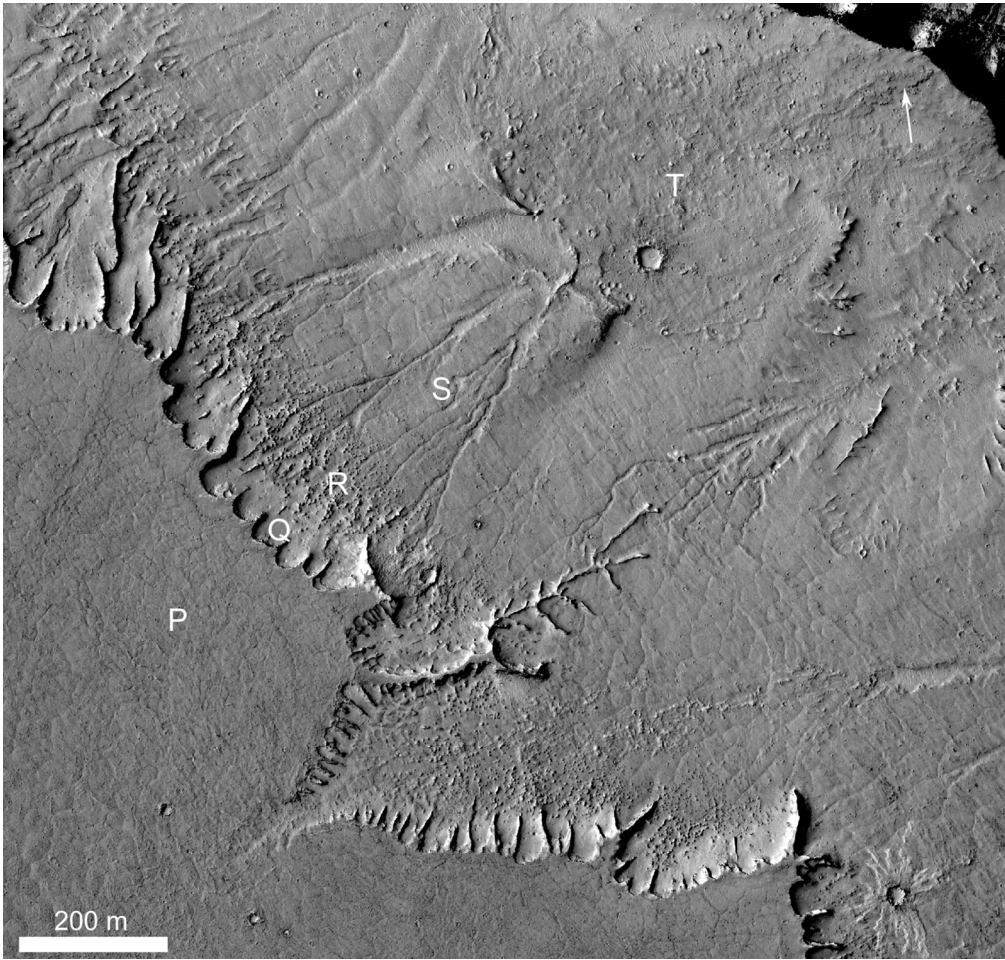


Figure 11
152x145mm (300 x 300 DPI)

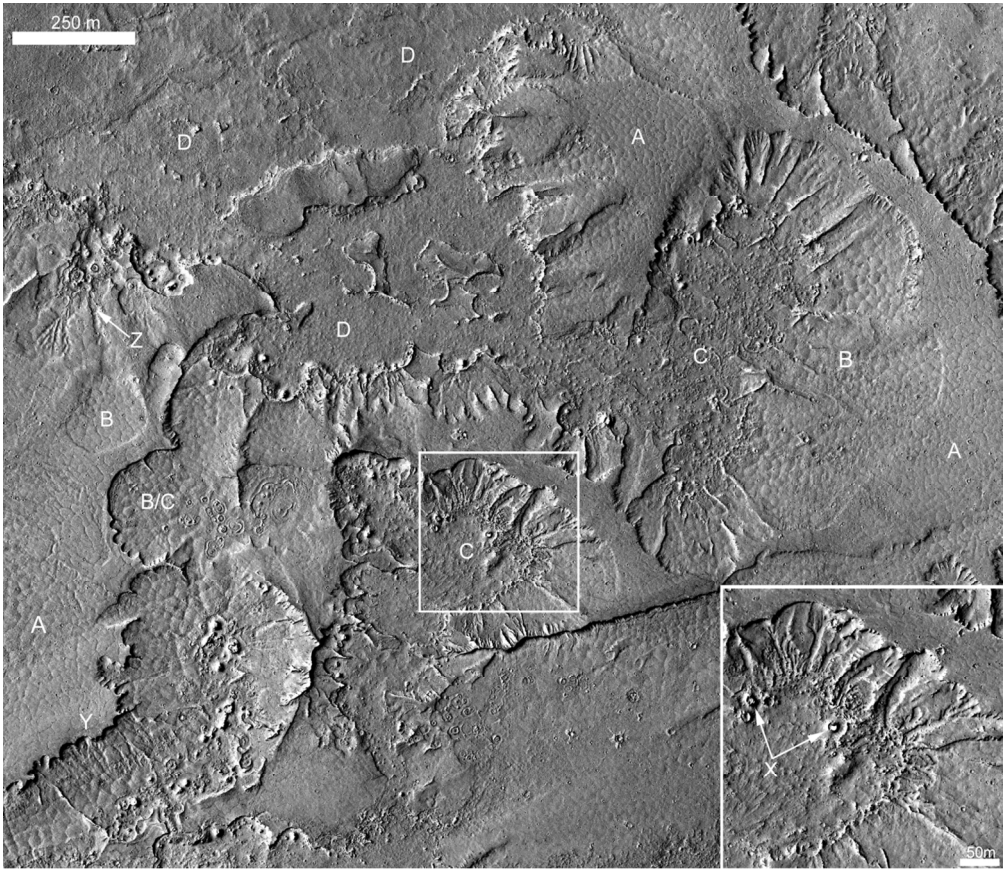


Figure 12
129x111mm (300 x 300 DPI)

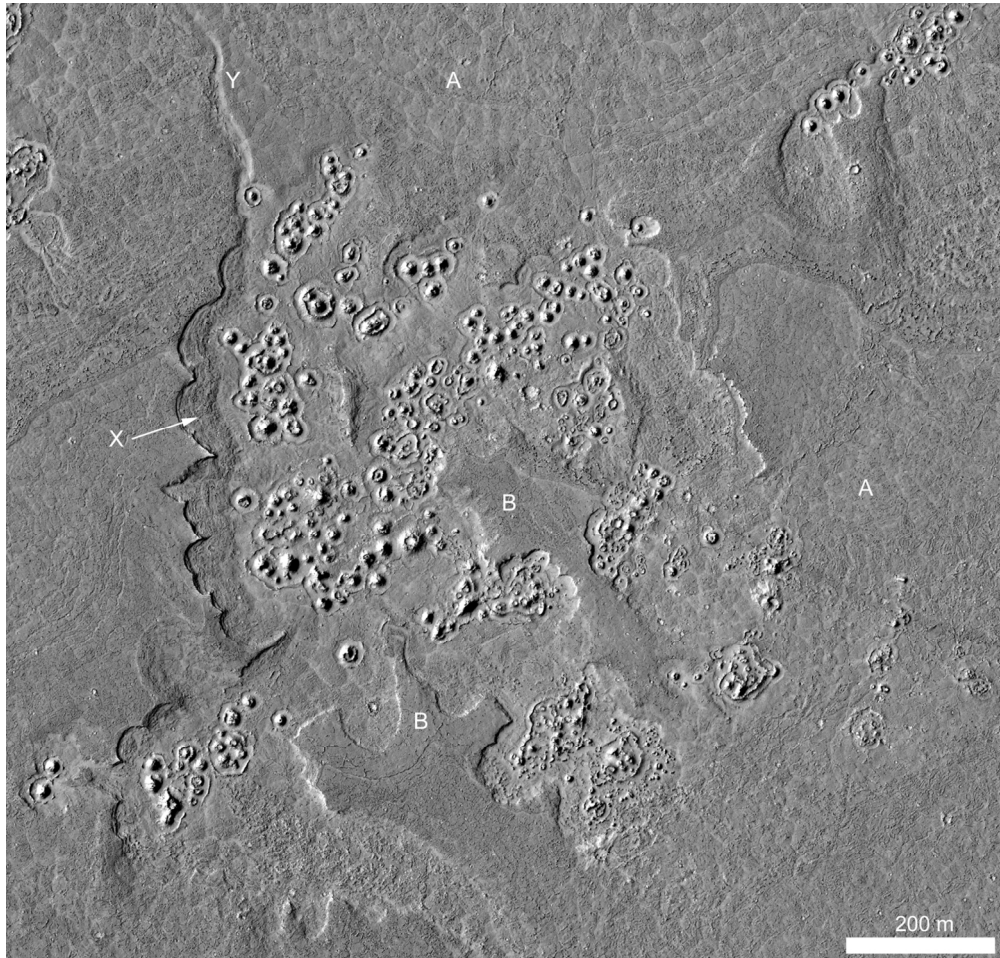


Figure 13
143x136mm (300 x 300 DPI)

Landform (morphology)	Periglacial interpretation	Indicative of liquid water?	Selected references	Alternative, dry interpretation	Alternative, dry interpretation References
Polygonally patterned ground	Thermal contraction polygons: (1) ice-wedge polygons (2) sand-wedge polygons (3) sublimation polygons	(1) yes (2) no (3) no	(1) (Seibert and Kargel, 2001) (2,3) (Levy et al., 2009a; Levy et al., 2010)	Desiccation cracks	(El Maarry et al., 2010)
Alternating dark and bright stripes	Sorted and unsorted stripes	yes (?)	(Hauber et al., 2011a; Hauber et al., 2011b; Mangold, 2005)	N/A	N/A
Clastic stripes	Sorted stripes	yes	(Gallagher and Balme, 2011; Gallagher et al., 2011)	N/A	N/A
Clastic circles, labyrinths and "rubble piles"	Sorted patterned ground	yes	(Balme et al., 2009; Gallagher and Balme, 2011; Gallagher et al., 2011)	Gravity-sorted clastic patterned ground enhanced by sublimation	(Heet et al., 2009; Levy et al., 2009a; Mellon et al., 2008)
Clastic lobes	Solifluction lobes	yes	(Gallagher and Balme, 2011; Gallagher et al., 2011; Johnsson et al., 2011)	N/A	N/A
Viscous flow features	Rockglaciers, or Debris-covered glaciers	no	(Head et al., 2010; Squyres, 1978; Squyres, 1979)	Aeolian deposits	(Zimbelman et al., 1989)
Small-scale valleys	Supra- and proglacial valleys	yes	(Dickson et al., 2009; Fassett et al., 2010)	N/A	N/A
Scalloped depressions	Thermokarst (melt)	yes	(Soare et al., 2007; Soare et al., 2008)	'Cryokarst' (Sublimation)	(Lefort et al., 2009; Morgenstern et al., 2007; Ulrich et al., 2010)
Mounds with pitted or fractured top	Pingos	yes	(Burr et al., 2009; Dundas et al., 2008; Page and Murray, 2006; Soare et al., 2005)	(1) Erosional remnants (2) Volcanic "rootless cones"	(1) (e.g., Burr et al., 2009; Dundas and McEwen, 2010) (2) (e.g., Jaeger et al., 2007; Lanagan et al., 2001)
Gullies	Erosion by fluvial or debris flow processes	yes	(Malin and Edgett, 2000); (Costard et al., 2002)	Dry mass wasting CO ₂ erosion	(Bart, 2007; Treiman, 2003) (Musselwhite et al., 2001)
Recurring slope lineae	Seepage of thaw liquid from buried deposits	yes	(McEwen et al., 2011)	N/A	N/A

1 Table 1.